Electrical Engineering
https://doi.org/10.1007/s00202-024-02789-8

ORIGINAL PAPER

Applicability of MMKE alongside statistical assessment in RESs and SVC-based power networks to solve the ORPD problem in load-varying scenarios

Sabyasachi Gupta[1] · Tushnik Sarkar[1] · Chandan Paul[1] · Susanta Dutta[1] · Provas Kumar Roy[2]

Received: 31 January 2024 / Accepted: 5 October 2024

Abstract
This paper attempts to solve the optimal reactive power dispatch (ORPD) problem on an IEEE 30-bus and IEEE 118 bus experimental networks. The traditional network is first countered, and then renewable energy sources including solar photovoltaic (PV) sources, wind power (WP), and tidal power (TP) are integrated with the traditional network. Both single and multiple type objective functions are investigated in this work. Lessening active power loss (APL), reducing the voltage stability index, lowering aggregated voltage deviation (AVD), and concurrently lowering AVD and APL are among the objectives. There are twenty two cases altogether between the three test modules. In conjunction with the test setup, SVC is being used in Cases 5–8, Cases 13–16 and Cases 20–22. The objectives have been accomplished by the application of the MMKE method, whose performance has been compared to that of other optimization algorithms documented in recent ORPD studies. The study includes situations with both constant load demand and uncertainly fluctuating load demand. The unknown WP, PV power, TP, and load demand are all estimated using the appropriate probability density functions. Monte Carlo simulations are used to develop uncertain scenarios with variable load demand, wind speed, solar irradiance, and tidal discharge rate. The number of scenarios is then whittled down to a reasonable quantity that does, in fact, reflect real-world circumstances using the backward reduction algorithm. The experiment results demonstrate that the MMKE can solve ORPD difficulties far more effectively than the optimization techniques found in the most recent ORPD literature, based on a variety of analysed instances. The Friedman test has been employed to statistically validate the effective performance of MMKE. A noteworthy result in the ORPD problem is that the application of SVC enhances power network performance.

Keywords Friedman test · Multi-trial vector based monkey king evolution (MMKE) · Optimal reactive power dispatch (ORPD) · Renewable energy sources (RESs) · Static VAr compensator (SVC)

✉ Tushnik Sarkar
tushnik.sarkar@bcrec.ac.in

Sabyasachi Gupta
sabyasachigupta@gmail.com

Chandan Paul
chandan815@rediffmail.com

Susanta Dutta
susanta.dutta@bcrec.ac.in

Provas Kumar Roy
roy_provas@yahoo.com

[1] Department of Electrical Engineering, Dr.B C Roy Engineering College, Durgapur, West Bengal, India

[2] Department of Electrical Engineering, Kalyani Government, Kalyani, West Bengal, India

Abbreviations

ORPD	Optimal reactive power dispatch
MMKE	Multi-trial vector based monkey king evolution
BRA	Backward reduction algorithm
PV	Photo voltaic
TP	Tidal power
OFs	Objective functions
PDF	Probability density functions
WS	Wind speed
ι	Scale factor for wind speed PDF
$\varkappa$	Shape factor for wind speed PDF
v_{in}	Turbine's cut-in speed
v_{r}	Turbine's rated speed
v_{out}	Turbine's cut-out speed
P_{wr}	Rated output of the wind turbine

Published online: 02 November 2024

$G_{n(\mathrm{pq})}$	Transmission line's transfer conductance
ϕ_{pq}	Voltage angle between bus p and q
λ	Multi-objective penalty factor
P_L and Q_L	Active and reactive power demand respectively
P_{G} and Q_{G}	Active and reactive power of generation respectively
g_{cd} and h_{cd}	Conductance and susceptance, respectively of the line connected between the cth bus and dth bus
φ_{cd}	Admittance angle of transmission line connected between the cth and the dth bus
$P_{Gb}^{\min}$, $P_{Gb}^{\max}$	Lower and upper bounds of active power generation, respectively, of the bth bus
$V_{\mathrm{Lb}}^{\min}$, $V_{\mathrm{Lb}}^{\max}$	The smallest and highest voltages, respectively, of the bth load bus
$T_b^{\min}$, $T_b^{\max}$	Bottom and extreme tap setting limits, respectively, of the bth regulating transformer
N_P	Quantity of generating buses
N_{LT}	The number of the transmission line
N_{sc}	The number of shunt compensators
EPU	Evaluating and population updating
MKE-TVP	Monkey king evolution trial vector producer
RTVP	Random trial vector producer
BHA	Best-history archive
RESs	Renewable energy sources
SVC	Static VAr compensator
FACTS	Flexible AC transmission system
WP	Wind power
APL	Active power loss
VSI	Voltage stability index
AVD	Aggregated voltage deviation
SI	Solar irradiance
ε	Average solar irradiance
λ	Solar irradiance's standard deviation
P_{nm}	Nominal output power of a PV unit
I_{st}	Standard solar irradiance
I_{c}	Critical irradiance point
τ	Location factor of tidal discharge rate
γ	Scale factors of tidal discharge rate
ρ	Water density (kg/m^3)
g	Gravity acceleration (m/s^2)
q_{tidal}	Water discharge value (m^3/s) across the turbine
η	Turbine efficiency
h	Distance between high and low water levels
$V_{\mathrm{Gb}}^{\min}$, $V_{\mathrm{Gb}}^{\max}$	Respectively, lower and upper voltage limits, for the b^{th} generator bus
$Q_{\mathrm{Gb}}^{\min}$, $Q_{\mathrm{Gb}}^{\max}$	Respective minimum and maximum reactive power generation margins of the bth bus
${S_{Lb}}^{\min}$, $S_{Lb}^{\max}$	The least apparent power flow and extreme apparent power flow limit respectively, of the bth branch
$Q_{CCbb}^{\min}$, $Q_{\mathrm{Cb}}^{\max}$	Minimum and maximum reactive power injection limits, respectively, of the bth shunt compensator
N_{BL}	The number of load buses
N_{T}	The number of regulating transformers
OBL	Oppositional based learning
TVP	Trial vector producer
BTVP	Best-history trial vector producer
WBD	Winner-based distribution

1 Introduction

Optimal reactive power dispatch which is supplement of traditional active power dispatch belongs to reactive power management scheme. Its prime aim is to enhance the performance and sustainability of the entire power system operations. In this regard, shunt compensation elements, tap changing transformers are used. To achieve improved solutions generator set points modified. ORPD is also crucial for better security and economy of power system operation. Indeed, resolving ORPD boosts the working of the power network by accomplishing some predefined objective functions like reduction in APL, AVD etc. To achieve these, appropriate value selection of some discrete variables (transformer and reactive bank taps) and some continuous variables (generators voltage set points) are the essential factors of the ORPD issue [1–3]. The most favourable modifications must be made to these control variables which include the distribution of the VAr shunt compensator, the tap settings of the transformers, the voltages of the generator buses, etc. [4, 5].

It is becoming more and more tempting in today's power sectors to integrate RESs into the current power grid for the sake of sustainability. Common RESs are Solar PV units, Wind units, Tidal Powers and Hydro powers. However the nature of output power from RESs is quite fluctuating, which increases the difficulty of solving ORPD [6].

Because of developments in power electronic technology, flexible AC transmission system (FACTS) tools-such as flexible, stable, and dependable VAr (reactive power) compensators-are being used more and more to address ORPD issues. FACTS was rarely used in ORPD problems in the past, but scientific discoveries in the last few years have rekindled interest in this field [7].

Typically, the main aims of resolving the ORPD issues are to reduce AVD which improves the voltage profile, decrease APL, improve the VSI etc. Although conventional optimization approaches like dynamic programming and linear programming have been studied in the literature, their performance is poor because ORPD issues contain non-differentiable OFs. Because these methods needed more iterations to yield results, they took longer duration to complete. They were more often coming up with local solutions than global ones. These traditional optimization techniques were unable to handle the complex, nonlinear nature of the ORPD problem.

It is noteworthy that the formulated problem in ORPD is nonlinear and non-convex by character. Numerous approaches and methods have been employed in the hunt for solutions to the ORPD in order to deal with this issue in an efficient and productive manner. More advanced optimization techniques have been developed continually to overcome the shortcomings of previous approaches to solving the ORPD problem. These techniques are currently being used to a variety of conventional and non-conventional [8, 9] power system applications, including the ORPD problem [10, 11]. To address ORPD difficulties, metaheuristic techniques are now being developed and applied with positive outcomes [12].

Here, in Table 1 few evidences from literature are presented in order to give a brief summary of the current status of the ORPD study. Several single OFs, including AVD reduction, lowering APL, VSI augmentation, operational cost minimization, fuel cost reduction, emission reduction, and also combining more OFs into a multi-OF, have been achieved through numerous optimization techniques. The data in Table 1 indicates that research on ORPD has not yet achieved its zenith, even in 2023, despite the greatest efforts of some researchers to enhance ORPD solutions. Nearly five years' worth of ORPD studies are compiled in Table 1 which, upon statistical analysis, reveals that 28 studies, out of 35, had selected the IEEE30 bus as their test network. According to Table 1, it shows that the IEEE 30-bus network was given preference over other IEEE bus systems. Counting the OFs considered in those studies, we find that 24 of them decided to lower AVD as an OF, and reducing APL as another OF. Accordingly, the most frequent OF in ORPD appears to be the decline in APL and AVD.

Since Table 1 indicates that the IEEE 30 bus network is a very common choice for studying ORPD issues, the present research efforts to tackle the ORPD problem on the IEEE 30 bus test power network to achieve minimum APL, AVD and VSI which are the most commonly chosen OFs, as indicated in Table 1. Afterword, some case studies have been carried out on IEEE 118-bus network which is much more complicated than IEEE 30 bus system. It is done to verify the effectiveness of the proposed optimization tool to accomplish highly complex system.

Based on the kind of required load, chosen test setups, and selected OFs, this research consists of 16 unique cases which are divided into two modules. In the first module, fixed load configured experiments are being carried out without consideration for RESs. While the first four cases in this module do not employ SVC, the final four cases are considered with SVC. The same methodology is used in the second module, *i.e.* the last four cases use SVC, whereas the first four cases do not. RESs are added to the test setup in the second module and the tests are carried out under various load scenarios. Formation of several load scenarios are performed in second test module which is not done in module one. 25 realistic scenarios are created using MCS and BRA, over which the testing in the second module is carried out. Replicating the events that occur in real power networks as closely as possible is the aim of the scenario creation.

In order to achieve the goals of the current ORPD study, MMKE algorithm is being used [44]. Multi-evolutionary techniques have been included into the monkey king evolution (MKE) [45] algorithm to create the MMKE algorithm. A Chinese mythological story served as the inspiration for MKE. Since the MKE algorithm only has one search method to address the problem, it performs badly when presented with a range of challenges. However, because MMKE mixes several techniques with MKE, it has overcome the shortcomings of its predecessor. The optimal power flow problem had been effectively solved by MMKE in literature [44].

Testing over the several considered cases and comparing the findings with published works in the literature on the same experimental platform establish that MMKE is superior to other current optimization algorithms for achieving effective ORPD solutions. The current results further demonstrate that the use of SVC improves system performance.

2 Model: SVC and RESs

2.1 Modelling of SVC

Figure 1 represents basic SVC structure. The equivalent susceptance is represented by

$$B_{\text{eq}} = B_L(\lambda) + B_C \tag{1}$$

where,

$$B_L(\lambda) = -\frac{1}{\omega L}\left(1 - \frac{2\lambda}{\pi}\right) \varsigma\ B_C = \omega \times C \tag{2}$$

Table 1 Various ORPD studies from literature

References	Year	Used algorithm for resolving ORPD	Benchmark functions	IEEE 14-bus system	IEEE 30-bus system	IEEE 39-bus system	IEEE 57-bus system	IEEE 114-bus system	IEEE 118-bus system	IEEE 300-bus system	Reducing APL	AVD diminution	VSI enrichment	Cost cutting	Lessening emission	Effects of uncertainty
[13]	2019	Modified sine cosine algorithm			✓						✓	✓	✓			
[14]	2019	Success history based adaptive differential evolution			✓		✓				✓	✓				
[15]	2019	Hybrid artificial physics-particle swarm optimization			✓		✓		✓		✓	✓	✓			
[16]	2019	Improved antlion optimization algorithm			✓		✓		✓		✓	✓	✓			
[17]	2019	Modified salp swarm algorithm			✓			✓			✓	✓				
[18]	2019	Enhanced grey wolf optimizer			✓						✓	✓				✓

Table 1 continued

References	Year	Used algorithm for resolving ORPD	Benchmark functions	IEEE 14-bus system	IEEE 30-bus system	IEEE 39-bus system	IEEE 57-bus system	IEEE 114-bus system	IEEE 118-bus system	IEEE 300-bus system	Reducing APL	AVD diminution	VSI enrichment	Cost cutting	Lessening emission	Effects of uncertainty
[2]	2020	Fractional-order Darwinian particle swarm optimization			✓		✓				✓	✓				
[11]	2020	Chaotic Bat algorithm		✓		✓	✓		✓	✓	✓	✓	✓			
[19]	2020	Marine predators' algorithm			✓						✓	✓				✓
[20]	2020	Improved social spider optimization algorithm	✓		✓				✓		✓	✓	✓			
[21]	2020	Artificial bee colony algorithm			✓		✓				✓	✓	✓			
[22]	2020	Water wave optimization			✓						✓					
[23]	2020	Jaya algorithm		✓	✓						✓					

Table 1 continued

References	Year	Used algorithm for resolving ORPD	Benchmark functions	IEEE 14-bus system	IEEE 30-bus system	IEEE 39-bus system	IEEE 57-bus system	IEEE 114-bus system	IEEE 118-bus system	IEEE 300-bus system	Reducing APL	AVD diminution	VSI enrichment	Cost cutting	Lessening emission	Effects of uncertainty
[24]	2021	Hybrid grey wolf optimization and particle swarm optimization		✓	✓				✓		✓	✓				
[25]	2021	Improved slime mould algorithm	✓				✓		✓	✓	✓					
[26]	2021	Modified pathfinder algorithm					✓		✓		✓					
[27]	2021	Improved Heap-based optimizer			✓		✓		✓		✓	✓	✓			
[28]	2021	Artificial ecosystem optimization			✓				✓	✓	✓	✓	✓			
[29]	2021	Sun flower optimization			✓						✓		✓			

Table 1 continued

References	Year	Used algorithm for resolving ORPD	Benchmark functions	IEEE 14-bus system	IEEE 30-bus system	IEEE 39-bus system	IEEE 57-bus system	IEEE 114-bus system	IEEE 118-bus system	IEEE 300-bus system	Reducing APL	AVD diminution	VSI enrichment	Cost cutting	Lessening emission	Effects of uncertainty
[30]	2021	Hybridization of genetic particle swarm optimization algorithm with symbiotic organisms search algorithm			✓						✓	✓	✓			
[31]	2021	Dragonfly optimization algorithm			✓						✓					
[32]	2022	Chaotic turbulent flow of water-based optimization			✓		✓				✓	✓				
[33]	2022	Continuous Ant Colony-based Differential Evolution			✓		✓				✓		✓			

Table 1 continued

References	Year	Used algorithm for resolving ORPD	Benchmark functions	IEEE 14-bus system	IEEE 30-bus system	IEEE 39-bus system	IEEE 57-bus system	IEEE 114-bus system	IEEE 118-bus system	IEEE 300-bus system	Reducing APL	AVD diminution	VSI enrichment	Cost cutting	Lessening emission	Effects of uncertainty
[34]	2022	Teaching and learning based optimization		✓	✓		✓				✓			✓		
[35]	2022	Artificial hummingbird algorithm		✓		✓					✓	✓				✓
[36]	2022	Coronavirus Herd Immunity Optimizer			✓		✓				✓		✓			
[37]	2022	Dynamic exploitation Gaussian barebones bat algorithm		✓			✓		✓		✓	✓	✓			
[38]	2022	Modified jellyfish optimizer			✓						✓	✓	✓			✓
[39]	2022	Improved aquila optimization		✓	✓		✓		✓		✓	✓	✓			

Table 1 continued

References	Year	Used algorithm for resolving ORPD	Benchmark functions	IEEE 14-bus system	IEEE 30-bus system	IEEE 39-bus system	IEEE 57-bus system	IEEE 114-bus system	IEEE 118-bus system	IEEE 300-bus system	Reducing APL	AVD diminution	VSI enrichment	Cost cutting	Lessening emission	Effects of uncertainty
[40]	2022	Hybrid fuzzy evolutionary algorithm		✓							✓					✓
[6]	2023	Modified artificial hummingbird algorithm			✓						✓	✓	✓			✓
[3]	2023	African vultures optimization			✓		✓		✓		✓	✓		✓		
[41]	2023	Augmented social network search			✓		✓		✓		✓	✓	✓			
[42]	2023	Enhanced Jaya and artificial ecosystem-based optimization			✓		✓				✓	✓				
[43]	2023	Improved barnacles Mating optimizer					✓				✓					

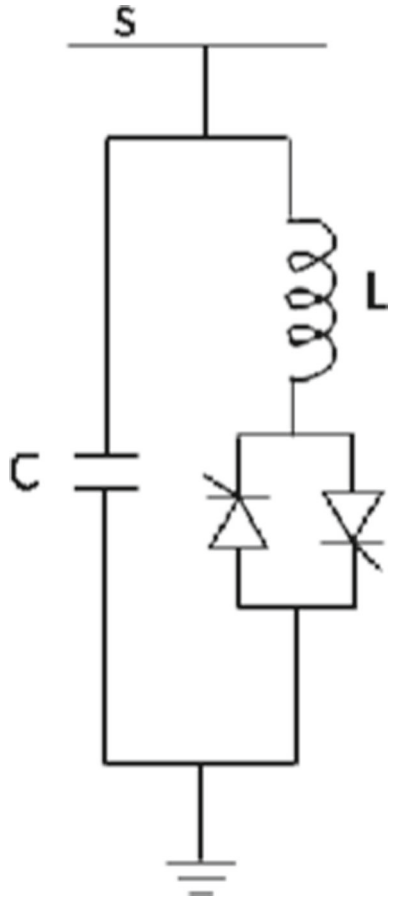

Fig. 1 Basic SVC structure

The injected reactive power at bus s, is given by:

$$Q_{\mathrm{SVC}} = -V_s^2 B_{\mathrm{SVC}} \tag{3}$$

The constraint on the reactive power at bus s is

$$B_{\mathrm{SVC}}^{\min} \le B_{\mathrm{SVC}} \le B_{\mathrm{SVC}}^{\max}. \tag{4}$$

2.2 WP model

Weibull PDF [46, 47], using its parameters scale factor (ι) and shape factor ($\varkappa$), gives a fair sketch of the variation in WS (v m/s) as:

$$f(v) = \left(\frac{\varkappa}{\iota}\right) \times \left(\frac{v}{\iota}\right)^{\varkappa-1} \times \left(e^{-(\frac{v}{\iota})^{\varkappa}}\right) \qquad 0 < v < \infty \tag{5}$$

The power output of a WT is presented in equation (6) in terms of the cut-in speed v_{in}, rated speed v_r, cut-out speed v_{out}, and rated output of the wind turbine (WT) P_{wr}.

$$P_w(v) = \begin{cases} 0 & for\ v < v_{\mathrm{in}}\ and\ v > v_{\mathrm{out}} \\ P_{\mathrm{wr}}\left(\frac{v - v_{\mathrm{in}}}{v_{\mathrm{r}} - v_{\mathrm{in}}}\right) & for\ v_{\mathrm{in}} \le v \le v_{\mathrm{r}} \\ P_{\mathrm{wr}} & for\ v_{\mathrm{r}} < v \le v_{\mathrm{out}} \end{cases} \tag{6}$$

Now, the possibility of WP in diverse WS zones can be determined by:

$$f(P_w)\big|_{P_w=0} = 1 - \exp\left[-\left(\frac{v_{\mathrm{in}}}{\iota}\right)^{\varkappa}\right] + \exp\left[-\left(\frac{v_{\mathrm{out}}}{\iota}\right)^{\varkappa}\right] \tag{7}$$

$$f(P_w)\big|_{P_w=P_{\mathrm{wr}}} = \exp\left[-\left(\frac{v_r}{\iota}\right)^{\varkappa}\right] - \exp\left[-\left(\frac{v_{\mathrm{out}}}{\iota}\right)^{\varkappa}\right] \tag{8}$$

$$\begin{aligned} f(P_w)\big|_{0<P_w<P_{\mathrm{wr}}} = {} & \left[\frac{\varkappa \times (v_r - v_{\mathrm{in}})}{\iota^{\varkappa} \times P_{\mathrm{wr}}}\right] \times \left[v_{\mathrm{in}} + \left(\frac{P_w}{P_{\mathrm{wr}}}\right)(v_r - v_{\mathrm{in}})\right]^{\varkappa-1} \\ & \times \exp\left[-\left(\frac{v_{\mathrm{in}} + \left(\frac{P_w}{P_{\mathrm{wr}}}\right) \times (v_r - v_{\mathrm{in}})}{\iota}\right)^{\varkappa}\right] \end{aligned} \tag{9}$$

2.3 PV model

The PV unit transforms solar energy into electrical energy. Together with other environmental factors, the SI level affects power output. As the distribution of probability of SI is very much resembled to the log normal PDF L(I) (I: denotes SI) [46, 48], SI is often estimated using L(I) and it is presented as:

$$L(I) = \frac{1}{I\lambda\sqrt{2\pi}} \exp\left(\frac{-(\ln I - \varepsilon)^2}{2\lambda^2}\right) \quad , \quad I > 0 \tag{10}$$

ε and λ, respectively, indicate the average and standard deviation of the I distribution.

The equation describing the link between SI and a PV unit's electrical output power is shown as:

$$P(I) = \begin{cases} P_{\mathrm{nm}} \frac{I^2}{I_{\mathrm{st}} I_c}, & for\ 0 < I < I_c \\ P_{\mathrm{nm}} \frac{I}{I_{st}}, & for\ I \ge I_c \end{cases} \tag{11}$$

P_{nm}, I_{st} and I_c, respectively, indicate the nominal output power of a PV unit, standard SI, and critical irradiance point.

2.4 TP model

The behaviour of the fluctuations of TDR (q_{tidal}) is usually modelled using Gumbel PDF [49], which is expressed as follows:

$$f\left(q_{\text{tidal}}\right)=\left(\frac{1}{\gamma}\right)\times e^{\left(\frac{q_{\text{tidal}}-\tau}{\gamma}\right)}\times e^{-e^{\left(\frac{q_{\text{tidal}}-\tau}{\gamma}\right)}} \tag{12}$$

where, with values of 220 and 24.52, respectively, τ and γ denote the location and scale factors of the TDR under consideration.

The tidal power plant has been displayed in Fig. 2. The output power of the tidal unit can be mathematically modelled as shown in equation (13) [49]

$$P_{\text{tidal}}(q_{\text{tidal}})=\rho g q_{\text{tidal}} h\eta \tag{13}$$

where ρ is the water density (kg/m^3), g is the gravity acceleration (m/s^2), q_{tidal} is the discharge value ((m^3/s)) across the turbine, η is the turbine efficiency and h is the difference between high and low water levels. These parameters of the system are set as h= 3.2 m, η =0.85, ρ=1025 kg/m^3 and g=9.81 (m/s^2).

3 Mathematical problem formulation

3.1 Objective function

Formation of single objectives include [50] the lessening of (a) APL and (b) AVD. The expression of the above-mentioned goals are given below:

3.1.1 APL

APL occurs in transmission lines due to inherent resistance. The APL that needs to be minimized is presented as follows:

$$Min\mathcal{F}_1=\sum_{n=1}^{N_L}G_{n(pq)}\left(V_p^2+V_q^2-2V_pV_q\cos\varphi_{pq}\right) \tag{14}$$

Buses p and q are connected by the nth line, which has a transfer conductance of $G_{n(\text{pq})}$. The total number of transmission lines is N_L. Voltage angle ϕ_{pq} exists between buses p and q.

3.1.2 AVD

In order to maintain a good voltage profile, AVD of the load buses ought to be held minimum. AVD is computed as:

$$\text{Min}\mathcal{F}_2=\sum_{l=1}^{N_B}|V_l-1| \tag{15}$$

V_l: lth load bus Voltage. N_B is the count of load buses.

3.1.3 VSI

Enhancing voltage stability is the third objective function. Voltage fluctuations leads to instability in voltage which has the potential to cause damage or even voltage collapse, either abruptly or gradually, in power networks. To prevent the voltage subside, VSI has to be improved. The VSI is presented as per following equations:

$$F_3=\min\left(L_{\max}\right)=\min\left(\max\left(L_j\right)\right)\ \forall\ j=1,2....,N_b \tag{16}$$

$$L_j=\left|1-\sum_{i=1}^{N_G}F_{ji}\frac{V_i}{V_j}\right|\ \forall\ j=1,2.....N_L \tag{17}$$

Here, L_j represents stability index of jth bus; $F_{ji}=-[Y_1]^{-1}[Y_2]$; Y_1 and Y_2 are network's Y_{BUS} sub-matrices.

3.1.4 Multi-objective function

Two or more objective functions in a multi-objective function can be addressed by combining them into a single function utilizing the Pareto front and weighted sum approaches. The weighted sum approach is used to analyse the multi-objective function in the suggested system in order to provide the following benefits.

a) It requires only one optimization run, making it computationally less expensive than the Pareto front technique.
b) It provides a single outcome that can be used to make decisions.optimization process.
c) It handles a single optimization problem, making it easier to execute than the Pareto front technique.

However, the proposed approach has some limitations as under.

a) The most effective responses may not be found throughout the whole objective space by it.
b) It might not be able to portray the trade-offs made between different goals with enough accuracy.

Three single-objective functions namely, active power loss (APL), aggregated voltage deviation (AVD), and voltage stability index (VSI) are individually minimized in the suggested systems. Furthermore, to evaluate the effectiveness of the suggested technique in a multi-objective environment, APL with AVD and APL, AVD with VSI are minimized concurrently. A penalty factor (λ1) and (λ2) are applied to the multi-objective functions in order to raise the priority level of the APL, AVD, and VSI. The multi-objective function ($F3$ and $F4$) is represented mathematically in (18) and (19) .

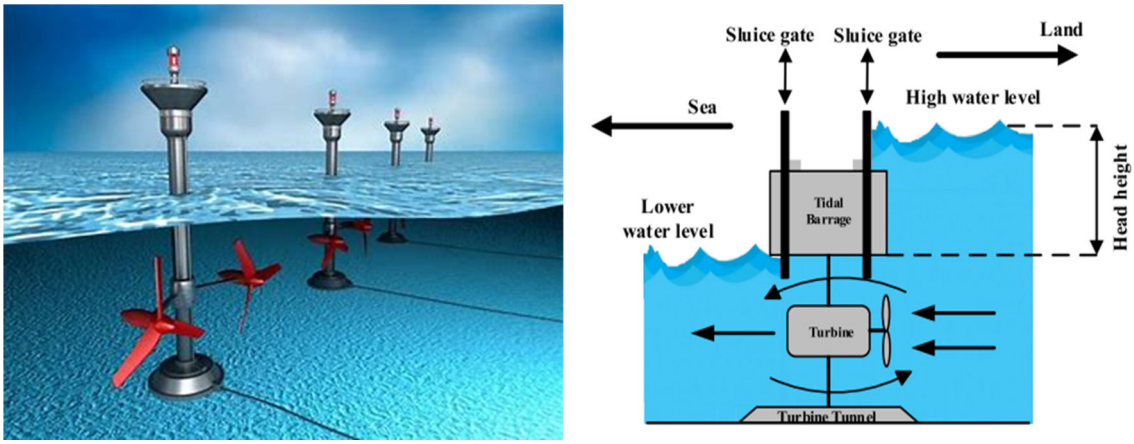

Fig. 2 Tidal power plant

The linear concoction of APL and AVD has been used to create a multi-objective function [14] like follows:

$$\text{Min}\mathcal{F}_3 = APL + \lambda_1.(AVD) \tag{18}$$

$$\text{Min}\mathcal{F}_4 = APL + \lambda_1.(AVD) + \lambda_2.(VSI) \tag{19}$$

where $\lambda_1(= 100)$ and $\lambda 2(= 100)$ are termed as penalty factor.

3.2 Constraints

The ORPD with SVC devices are subject to the following constraints:

3.3 Equality constraints

Constraint (20) is a equation of power flow which is presented below:

$$\begin{cases} \sum_{c=1}^{N_s} (P_{Gc} - P_{Lc}) = \sum_{c=1}^{N_s} \sum_{d=1}^{N_s} V_c V_d \left(g_{cd} \cos\varphi_{cd} - h_{cd} \sin\varphi_{cd}\right) \\ \sum_{c=1}^{N_s} (Q_{Gc} - Q_{Lc}) = -\sum_{c=1}^{N_s} \sum_{d=1}^{N_s} V_c V_d \left(g_{cd} \sin\varphi_{cd} - h_{cd} \cos\varphi_{cd}\right) \end{cases} \tag{20}$$

where P_{Lc} and Q_{Lc} are the active and reactive power demand of the cth bus; P_{Gc} and Q_{Gc} are the active and reactive power of generation, respectively, of the cth bus; g_{cd} and h_{cd} are the conductance and susceptance, respectively, of the line connected between the cth bus and dth bus; φ_{cd} is the admittance angle of transmission line connected between the cth and the dth bus.

3.4 Inequality constraints

(i) Generator constraints:

$$\begin{cases} V_{Gb}^{\min} \le V_{Gb} \le V_{Gb}^{\max} \\ P_{Gb}^{\min} \le P_{Gb} \le P_{Gb}^{\max} \quad b \in N_P \\ Q_{Gb}^{\min} \le Q_{Gb} \le Q_{Gb}^{\max} \end{cases} \tag{21}$$

(ii) Load bus constraints:

$$V_{Lb}^{\min} \le V_{Lb} \le V_{Lb}^{\max} \quad b \in N_{BL} \tag{22}$$

(iii) Transmission line constraints:

$$S_{Lb} \le S_{Lb}^{\max} \quad b \in N_{LT} \tag{23}$$

(iv) Transformer tap constraints:

$$T_b^{\min} \le T_b \le T_b^{\max} \quad b \in N_T \tag{24}$$

(v) Shunt compensator constraints:

$$Q_{Cb}^{\min} \le Q_{Cb} \le Q_{Cb}^{\max} \quad b \in N_{sc} \tag{25}$$

where $V_{Gb}^{\min}$, $V_{Gb}^{\max}$ indicate, respectively, lower and upper voltage limits, for the bth generator bus; $P_{Gb}^{\min}$, $P_{Gb}^{\max}$ are the lower and upper bounds of active power generation, respectively, of the bth bus; $Q_{Gb}^{\min}$, $Q_{Gb}^{\max}$ are the respective minimum and maximum reactive power generation margins of the bth bus; $V_{Lb}^{\min}$, $V_{Lb}^{\max}$ are the smallest and highest voltages, respectively, of the bth load bus; $S_{\text{Lb}}{}^{\min}$, $S_{\text{Lb}}^{\max}$ are the least apparent power flow and extreme apparent power flow limit, respectively, of the bth branch; $T_b^{\min}$, $T_b^{\max}$ are the bottom and extreme tap setting limits, respectively, of the bth regulating transformer; $Q_{Cb}^{\min}$, $Q_{Cb}^{\max}$ are the minimum and

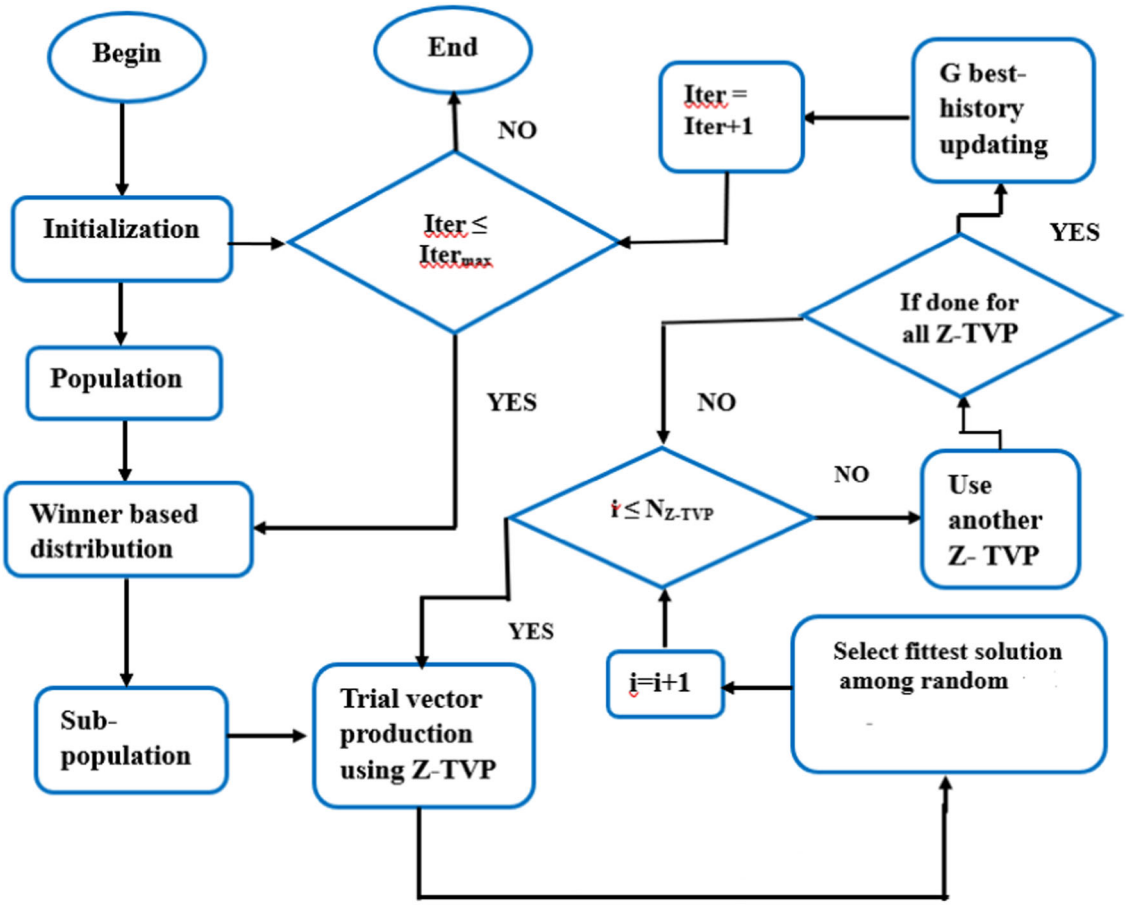

Fig. 3 Flowchart of MMKE

maximum reactive power injection limits, respectively, of the bth shunt compensator; N_P is the quantity of generating buses; N_{BL} represents load buses; N_{LT} is the number of the transmission line; N_T is the number of regulating transformers; N_{sc} is the number of shunt compensators.

4 Algorithm for optimization

4.1 Multi-trial vector-based monkey king evolution (MMKE)

The MMKE algorithm is composed of the subsequent essential steps: initialization, winner-based distribution (WBD), Multi-trial vector generation for MMKE, Population updating (EPU), Evaluation, and archiving [44] is described.

1. Initialization
   N monkeys (the beginning population) are randomly selected within the specified boundaries by

$$H_{ij} = H_{ij}^{\min} + r * \left(H_{ij}^{\max} - H_{ij}^{\min}\right) \quad \text{for } i = 1 \text{ to } N \text{ and } j = 1 \text{ to } m \tag{26}$$

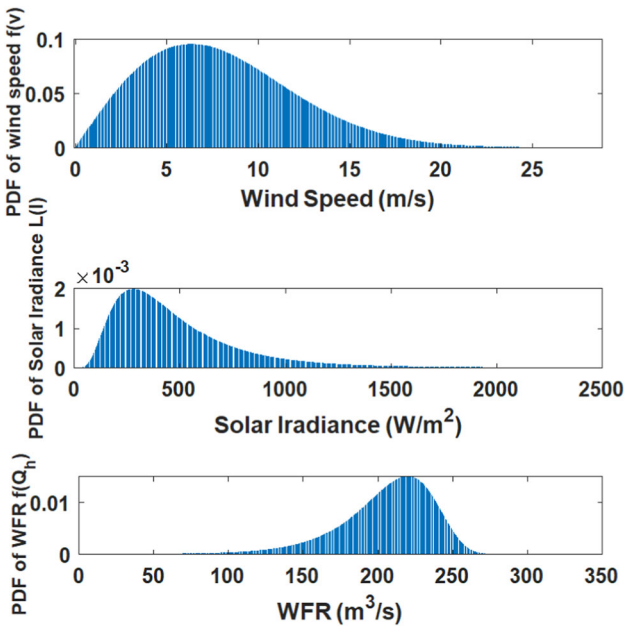

Fig. 4 Weibull-based WS PDF with $\iota = 10$ and $\varkappa = 2$, Lognormal-based SI (W/m^2) PDF with $\varepsilon = 6$ and $\lambda = 0.6$ and Gumbel-based TDR PDFs with $\tau = 220$, $\gamma = 24.52$

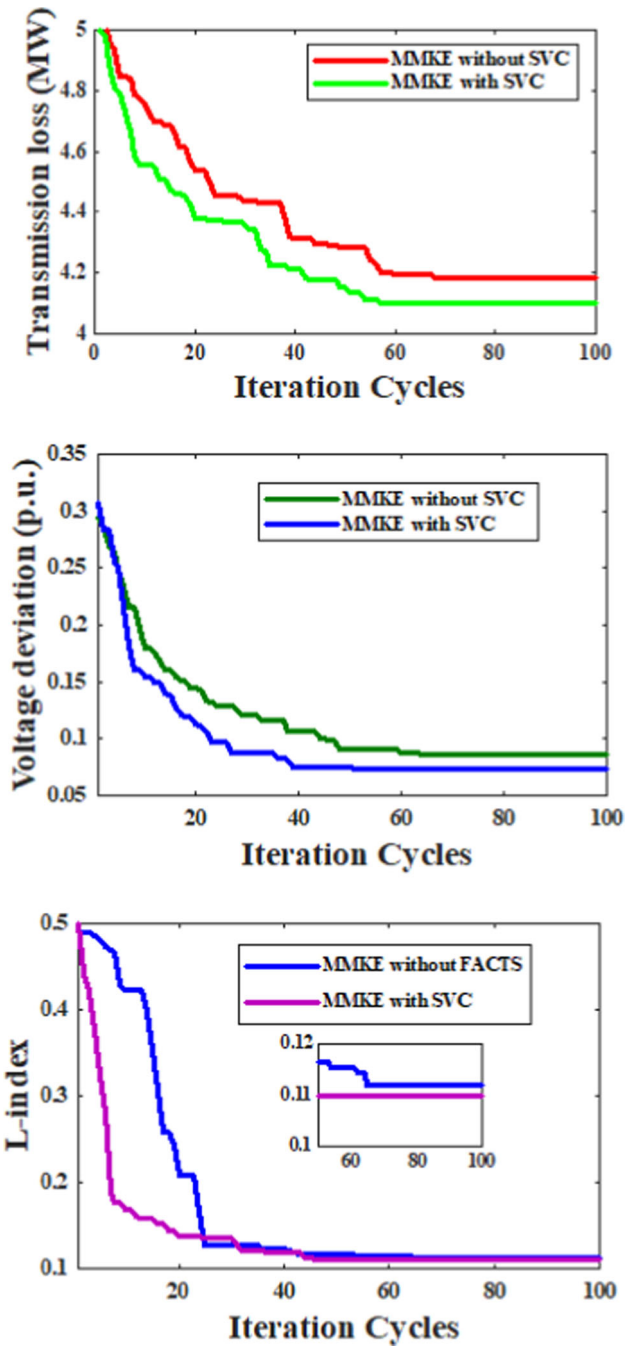

Fig. 5 Convergence characteristics of APL, AVD and VSI using MMKE with and without SVC

where the jth variable of the ith solution (monkey) for the problem under consideration has upper and lower bounds, respectively, denoted by $H_{ij}^{\max}$ and $H_{ij}^{\min}$; r is a random variable that ranges from 0 to 1. The dimensions of the analysed optimisation problem are m. The positions of N monkeys are included in the matrix $H_{N\times m}$. The monkey H_i has a fitness amount of $f(H_i(t))$ at tth generation.

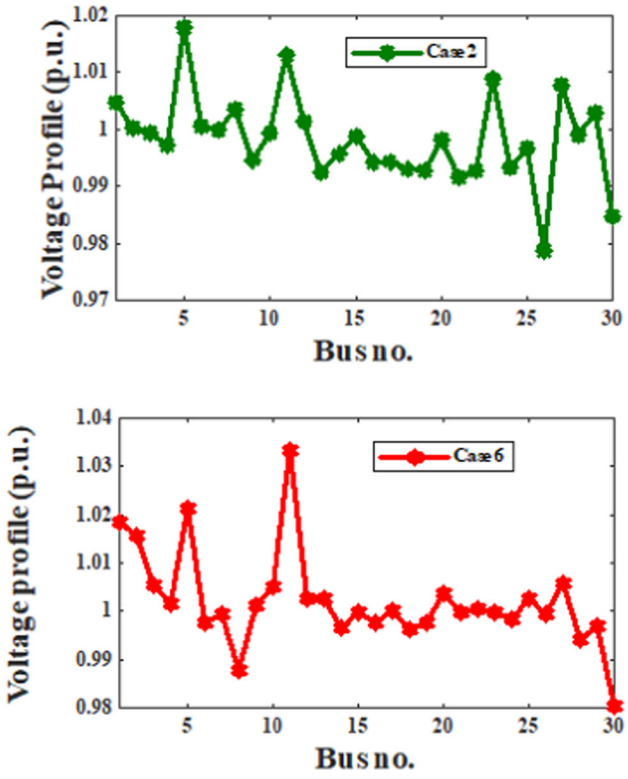

Fig. 6 Voltage deviations over load buses for case 2 and 6

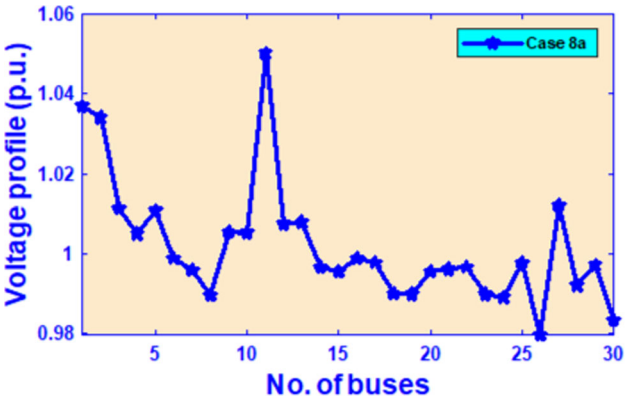

Fig. 7 Voltage deviations over load buses for Case 8a

2. Winner-based distributing (WBD)
There are k segments separating the entire generation. The trial vector producer (TVP) with the largest improvement for each section is selected first, superseding previous generations. The improved rate IR_{Z-TVP} for each TVP is computed as follows:

$$IR_{Z-\mathrm{TVP}} = \frac{\text{improved solutions}}{\text{function evolutions}} \tag{27}$$

The size of each TVP's sub-population is evaluated for the subsequent n generations utilising the reward rule allocation approach after the increased rates for all TVP

have been calculated. The results are shown as follows:

$$N_{Z-\mathrm{TVP}} = \begin{cases} 2\times\gamma\times N & \text{for TVP having larger rate of improvement} \\ \gamma\times N & \text{for different TVPs} \end{cases} \tag{28}$$

N is count of monkeys, $N_{Z-\mathrm{TVP}}$ is the sub-population size depending on TVP's improved rate and $\gamma = 0.25$ [44].

3. Multi-trial vector producing of MMKE
A combination of the following methods is used to propagate monkey H_i through all generations: (a) monkey king evolution trial vector producer (MKE-TVP), (b) best-history trial vector producer (BTVP) and (c) random trial vector producer (RTVP). The MKE-TVP encourages exploration potential by empowering participants to look for out novel solutions in their local community. One can take advantage of and get away from the regional optimum with BTVP. While TVP modifies its perceptive subpopulation, RTVP seeks to balance exploration and exploitation. In (29), the M and $\overline{M}$ are used to create the monkeys' evolved vector. M denotes a lower triangular matrix with elements set to one, and M's binary inverse is $\overline{M}$.

$$\begin{aligned} O_i^{M\mathrm{pop}}(t+1) &= M_i \times H_i^{M\mathrm{pop}} + \overline{M_i} \times V_i^{M\mathrm{pop}} \\ O_i^{B\mathrm{pop}}(t+1) &= M_i \times H_i^{B\mathrm{pop}} + \overline{M_i} \times V_i^{B\mathrm{pop}} \\ O_i^{R\mathrm{pop}}(t+1) &= M_i \times H_i^{R\mathrm{pop}} + \overline{M_i} \times V_i^{R\mathrm{pop}} \end{aligned} \tag{29}$$

where O_i^{Mpop}, O_i^{Bpop} and $O_i^{R\mathrm{pop}}$ indicate the developed candidate solution for $H_i^{M\mathrm{pop}}$, $H_i^{B\mathrm{pop}}$ and $H_i^{R\mathrm{pop}}$ ($i.e.$ for ith monkey) within sub-population MKE-TVP, BTVP and RTVP respectively; $V_i^{M\mathrm{pop}}$, $V_i^{B\mathrm{pop}} and V_i^{R\mathrm{pop}}$ are the mutated vector of MKE-TVP, BTVP and RTVP sub-populations, respectively, for ith monkey. (a)Monkey king evolution trial vector producer (MKE-TVP) The best monkey is selected from H as gbest for each generation and is kept in $\mathrm{gbest}^{\mathrm{pop}}$. To further shift any monkey H_i in sub-population $H^{M\mathrm{pop}}$, a coefficient of fluctuation ($FC = 0.7$) is employed; two randomly selected monkeys are $H_{r1}^{M\mathrm{pop}} and H_{r2}^{M\mathrm{pop}}$. Based on that $V_i^{M\mathrm{pop}}$, MKE-TVP creates a modified vector for ith monkey of $H^{M\mathrm{pop}}$ as follows:

$$\begin{aligned} V_i^{M\mathrm{pop}}(t+1) &= g\mathrm{best}^{\mathrm{pop}}(t) \\ &\quad + FC \times \left(H_{r1}^{M\mathrm{pop}}(t) - H_{r2}^{M\mathrm{pop}}(t)\right) \end{aligned} \tag{30}$$

Due to its additional exploratory nature in the early stages of development and its transition to unnecessary exploitative behaviour in the later stages of optimisation, this technique will yield universally accepted answers regarding the best monkey. (b) Best-history trial vector producer (BTVP) The MKE-TVP is more avaricious than this tactic. By avoiding early convergence and local optima catching, it closes a gap in MKE-TVP. Rather than using a single global best monkey, this strategy accounts for M recent finest monkeys that are preserved in the best-history archive (BHA). For ith monkeys inside sub-population $H^{B\mathrm{pop}}$ in BTVP, the modified vector $V_i^{B\mathrm{pop}}$ is created as follows:

$$\begin{aligned} V_i^{B\mathrm{pop}}(t+1) &= H_i^{Bh\mathrm{pop}}(t) \\ &\quad + C \times \left(H_{r1}^{B\mathrm{pop}}(t) - H_{r2}^{B\mathrm{pop}}(t)\right) \end{aligned} \tag{31}$$

In this case, the i^{th} monkey for BHA is $H_i^{Bh\mathrm{pop}}$; any two randomly selected monkeys from the subpopulation $H^{B\mathrm{pop}}$ are $H_{r1}^{B\mathrm{pop}}$ and $H_{r2}^{B\mathrm{pop}}$. The decreasing coefficient C is given by

$$C = \xi - (\xi - \rho) \times \left(\frac{(Mx.Ge - P.Ge)}{Mx.Ge}\right)^{\mu} \tag{32}$$

Here, $Mx.Ge$ is maximum generation; $P.Ge$ is present generation; $\xi = 0.001$, $\rho = 2$ [44] and $\mu = \log m$. (c) Random trial vector producer (RTVP)
RTVP balances exploration with exploitation. In RTVP, for ith monkey of sub-population $H^{R\mathrm{pop}}$, the $V_i^{R\mathrm{pop}}$ mutated vector is obtained as:

$$\begin{aligned} V_i^{Rpop}(t+1) &= H_i^{R\mathrm{pop}}(t) + F_i \\ &\quad \times \left(H_{r1}^{R\mathrm{pop}}(t) - H_i^{R\mathrm{pop}}(t)\right) \\ &\quad + F_i \times \left(H_{r2}^{R\mathrm{pop}}(t) - H_j^{Al\mathrm{pop}}(t)\right) \end{aligned} \tag{33}$$

Within sub-population $H^{R\mathrm{pop}}$, $H_i^{R\mathrm{pop}}$ is i^{th} monkey, $H_{r1}^{R\mathrm{pop}}$ and $H_{r2}^{R\mathrm{pop}}$ are respectively $r1$th and $r2$th random monkeys; $H_j^{Al\mathrm{pop}}$ is any arbitrary monkey belongs to $H \bigcup H^{Bh\mathrm{pop}}$; Scale factor F_i ranges from 0 to 1 [51].

4. Evaluating and population updating (EPU)
The fitness of the progeny is evaluated and contrasted with that of the progenitor monkeys as soon as one generation of monkeys matures. Only the most accomplished monkeys make up the following generation.
5. Archiving
In order to acquire high diversity over simple and composite problems, when low-quality monkeys are observed, they are preserved so that they might share their expertise with the monkeys of future generations. This can prevent the search being conducted near inferior animals or in unproductive places. It is possible for the archive to hold a maximum of N monkeys. The longer-living monkey is ejected when it surpasses N.

5 Simulation outcomes and comparisons for various cases

Using the MMKE technique, the simulation results for several ORPD case studies are presented in this part and are compared with earlier research [6]. The MATLAB platform is used to run entire simulations. As test systems, the IEEE 30-bus network and its modified structures have been chosen. A succinct summary of test system descriptions is given in Table 2.

Table 2 lists two test networks: one with a base configuration and the other with an updated configuration. There are now two test modules that can be categorize the research in general. Within two test modules, the present study can be broadly classified. For an equitable comparison, the test systems are selected based on the system utilized in [6]. In test module 1, only thermal generation is considered; in test module 2, RESs are introduced with an older test system. Table 3 displays the PDF details for WP, PV sources and TDR. The weibull-based WS PDF, the lognormal-based SI PDF and Gumbel-based TDR PDFs are displayed in Fig. 4 in accordance with the parameter values given in Table 3.

A total of 12 examples are investigated over these two test networks and are compiled in Table 4.

Test Module 1 examines Cases 1 through 8, whereas Module 2 looks into Cases 9 through 16. The first and second test modules can be divided into two parts: the SVC-integrated test network and the SVC-free network. To be more precise, examples 1–4 and 9–12 do not consider SVC, while cases 5–8 and 13–16 are examined while utilizing SVC with the test set up. With the exception of swing generators, the active power settings for generators in the context of optimization need to be carefully selected while staying within the generators' specified limits. These amounts are displayed in Table 19 (as an appendix) for cases 1–8 and cases 9–16. For each test configuration, there are four objectives. These include decreasing APL, minimizing AVD and VSI as single-objective situations, and lowering APL and AVD simultaneously as multi-objective cases.

5.1 1st Module

The test network for this module may be found in Table 2, under the "Base configuration" section. This test setup is used for Cases 1–8, and SVC combined with the test network is used for Cases 5–8. In this module, a network loading (constant) of 100% has been considered. The computed results for cases 1–4 and cases 5–8 are shown in Tables 5 and 6, respectively.

These tables show the optimal and extreme border values for each variable along with the estimated magnitudes of the objective quantities. A similar test network was used in [6], where the Modified Artificial Hummingbird Algorithm (MAHA) algorithm was employed. In this study, APL, AVD, and VSI are reduced as single OFs and APL and AVD are reduced simultaneously using the MMKE algorithm.

Important takeaways from Table 5 are:

- Using MMKE, APL is found to be 4.1811 (MW) in case 1, while it was found to be 4.5086 (MW) in [6]. Consequently, MMKE reduces APL by 0.3275 (MW) with respect to [6].
- The AVD in case-2, calculated with MMKE, is 0.0861 p.u., which is 0.0018 p.u. smaller than the AVD reported in [6].
- The VSI with MMKE in case-3 is 0.1107, while it was 0.1132 in [6]. Hence, in contrast to [6], MMKE reduces VSI by 0.0025.
- Considering simultaneous objectives, specifically APL and AVD, the results in case 4 are notable. Although Case 4's APL and AVD are higher than Cases 1 and 2, respectively, overall, Case 4's APL and AVD are superior to Cases 1 and 2.

The computational duration for each case is listed in the last row of this result. It shows that employing MMKE helps to achieve better results faster in addition to improving the optimization outcomes for examples 1–3 when compared to [6].

Table 6 displays the outcomes of the trials that were conducted while accounting for SVC with base setup. It demonstrates that:

- Case 5's computed APL value is 4.1001(MW), which is less than case 1's APL by 0.081(MW).
- For case 6, the computed AVD is 0.0739 (p.u.). By 0.0122 (p.u.), the AVD found in case 2 is higher than the AVD of case 6.
- In case 7, the VSI is computed as 0.1097 (p.u.). In case 7, the VSI is 0.001 (p.u.) less than the VSI found in case 3.
- In case 8, the multi-objective situation, the APL and AVD are 4.9305(MW) and 0.1025 (p.u.), respectively, which are better than those values in case 4.
- In Case 8a, APL, AVD and VSI are simultaneously minimized. The outcomes for APL, AVD and VSI are respectively 5.05 MW, 0.1208 p.u. and 0.1385 p.u.
- As mentioned earlier, SVC was added to the test configuration which was utilized for cases 1–4, and cases 5–8 have been conducted with this modified arrangement.

It is clear from the aforementioned results (cases 1 through 8) that the power network's employment of SVC significantly contributes to the ORPD issue's success.

Table 2 An overview of IEEE 30- bus system

Items	Quantity	Base configuration Details	Quantity	Adapted configuration Details
Buses	30	[6]	30	[6]
Branches	41	[6]	41	[6]
Thermal generators	6	Buses: 1 (swing), 2, 5, 8, 11 and 13	3	Buses:1 (swing), 2 and 8
Wind generators			2	Bus: 5, 13
Solar PV unit			1	Bus: 11
Tidal power			1	Bus: 13
Tap changing transformer	4	Branches: (6–9), (6–10), (4–12) and (28–27)	4	Branches: (6–9), (6–10), (4–12) and (28–27)
Control variables	19	bus voltages of all generator buses (6Nos.)	19	bus voltages of all generator buses (6Nos.)
		transformer tap setting (4Nos.) and compensation devices (9Nos.)		transformer tap setting (4Nos.) and compensation devices (9Nos.)
Load demand		283.4 MW, 126.2 MVAr		Variable
Range of load bus voltage	24	[0.95−1.05] p.u.	24	[0.95−1.05] p.u.
SVC			2	Branch location and rating optimized
Compensation devices	9	Buses: 10, 12, 15, 17, 20, 21, 23, 24 and 29	9	Buses: 10, 12, 15, 17, 20, 21, 23, 24 and 29

Table 3 Particulars of used PDFs for RESs

Specifications	WG	PV	TDR
PDF	Weibull	Lognormal	Gumbel
Parameters	$\xi = 10, \kappa = 2$	$\varepsilon = 6, \lambda = 0.6$	$\tau = 220, \gamma = 24.52$

The APL, AVD, and VSI minimization convergence characteristics with and without SVC consideration are shown in Fig. 5.

The curves in Fig. 5 make it evident how adding SVC to the power network improves system performance. Figure 6 shows the voltage variation throughout the every load bus for cases 2 and 6 whereas Fig. 7 depicts the load bus voltage deviations for Case 8a.

5.2 2nd Module

In this section of the experiment, eight cases (cases 9–16) are taken into consideration, as shown in Table 4. Of these, the first four cases (cases 9–12) are conducted over the test network without taking SVC into consideration, and the remaining cases (cases 13–16) are conducted over the test network with SVC. The test configuration utilized in this section is shown on the right-hand side of Table 2. The addition of RESs (WP, PV and Tidal power) to a conventional model is referred to as a "adapted configuration". Additionally, in this mode of experiment, the volatility of RESs and the unexpected nature of load have been handled through the process of scenario development and scenario downsizing [14]. In order to estimate uncertain load demand, the normal PDF with a mean of 70 and a standard deviation of 10 has been taken into account [14]. Uncertain WS, SI, and TWD estimated using Weibull, Lognormal, and Gumbel PDFs, respectively, at the time of scenarios formation. Since the sun is present for just approximately half of a 24-hour day, zero irradiance is assigned with a 50% chance during scenario development. 50% of the remaining choices are assigned to scenarios where the PV power contribution is not zero. The components of a single scenario are the load demand, WS, SI, and TWD.

First, a collection of 1000 scenarios is created by combining the 1000 Monte-Carlo choices for load demand, WS, SI, and TWD. Since handling 1000 possibilities is unmanageable, BRA [52] trimmed the 1000 situations to 25 scenarios. First, N_0 scenarios are taken into account with a probability associated with each scenario being ($\rho_0 = \frac{1}{N_0}$). A single possibility is eliminated following each BRA iteration in an attempt to lower the overall set of possible outcomes. The BRA reduces scenarios by taking the following actions:

1. **Initialization**
   - Create N_0 scenarios (S_i for $i = 1, 2, \ldots, N_0$). Currently: $N_0 = 1000$.

Table 4 Various case studies investigated in this study

Case	Single objective	Multi-objective	Considered objectives	Constraints	Test system
1	✓		APL minimization	Equality and non-equality	IEEE 30-bus
2	✓		AVD minimization	Equality and non-equality	
3	✓		VSI minimization	Equality and non-equality	
4		✓	Simultaneous minimization of APL and AVD	Equality and non-equality	
5	✓		APL minimization	Equality and non-equality	IEEE 30-bus
6	✓		AVD minimization	Equality and non-equality	incorporating SVC
7	✓		VSI minimization	Equality and non-equality	
8		✓	Simultaneous minimization of APL and AVD	Equality and non-equality	
8a		✓	Simultaneous minimization of APL, AVD andVSI	Equality and non-equality	
9	✓		APL minimization	Equality and non-equality	IEEE 30-bus
10	✓		AVD minimization	Equality and non-equality	incorporating wind, PV and Tidalenergy
11	✓		VSI minimization	Equality and non-equality	
12		✓	Simultaneous minimization of APL and AVD	Equality and non-equality	
13	✓		APL minimization	Equality and non-equality	IEEE 30-bus
14	✓		AVD minimization	Equality and non-equality	incorporating wind, PV and Tidal energy and SVC
15	✓		VSI minimization	Equality and non-equality	
16		✓	Simultaneous minimization of APL and AVD	Equality and non-equality	
17	✓		APL minimization	Equality and non-equality	IEEE 118-bus
18	✓		AVD minimization	Equality and non-equality	
19	✓		VSI minimization	Equality and non-equality	
20	✓		APL minimization	Equality and non-equality	IEEE 118-bus
21	✓		AVD minimization	Equality and non-equality	incorporating SVC
22	✓		VSI minimization	Equality and non-equality	

- At the beginning, the chance of every scenario is identical ($\rho_0 = \frac{1}{N_0}$).
  Determine the distance d_{ij} among each pair of sce-Step 3:
  narios. where $d_{ij} = \|S_i - S_j\|$.
- With d_{ij}, set up distance matrix D with starting dimension $N_0 \times N_0$ and diagonal elements $d_{ii} = 0$. Step 4:
- Allot a running variable $N_r = N_0$ and stopping criterion N_{ec}, indicates the count of final preferred scenarios.

2. **Looping events**

Step 1: Find least distance value (apart from self-distance $d_{ii} = 0$) from D. Suppose d_{mn} is least in D ($i.e.$ separation between m^{th} and n^{th} scenarios), and suppose scenarios $S_m and S_n$ having likelihoods of ρ_m and ρ_n respectively.

Step 2: If $\rho_m \geq \rho_n$, remove scenario n. Modify likelihood $\rho_m = \rho_m + \rho_n$.
Else, take away scenario m. Alter probability $\rho_n = \rho_m + \rho_n$.

Allocate $N_r = N_r - 1$.
reassess the matrix D, composed of distance between each pair of existing scenarios.

If $N_r > N_{ec}$,
jump to STEP 1 of reiterating.
Else, END.

Table 7, displays these 25 scenarios together with the corresponding probability.

Table 7 displays the load demand as % loading. Based on the situations presented in Table 7, the corresponding WP, PV, and HP are assessed and displayed in Table 8 using equations (6), (11), and (12), respectively.

The optimization procedure is then run separately for each scenario. After executing those algorithms, the values of the

Table 5 Simulation results of case studies with fixed loading (100%) for the IEEE 30-bus system (base configuration)

Control parameters	Min.	Max.	Case 1 [6]	Case 1 [MMKE]	Case2 [6]	Case 2 [MMKE]	Case 3 [6]	Case 3 [MMKE]	Case 4 [MMKE]
V1 (p.u.)	0.9	1.1	1.1	1.0907	1.0077	1.0048	1.0984	1.055	1.0385
V2 (p.u.)	0.9	1.1	1.0944	1.0813	0.9929	1.0002	1.0897	1.0461	1.0223
V5 (p.u.)	0.9	1.1	1.075	1.058	1.0691	1.018	1.0915	1.0237	1.0286
V8 (p.u.)	0.9	1.1	1.077	1.0596	1.007	1.0036	1.0903	1.0479	0.9811
V11 (p.u.)	0.9	1.1	1.1	1.0987	0.9973	1.013	1.0999	1.0641	1.0212
V13 (p.u.)	0.9	1.1	1.1	1.0997	1.0074	0.9926	1.0862	1.0149	1.0165
T11 (p.u.)	0.9	1.1	0.9961	1.001	1.0084	1.0311	1.0435	1.0618	1.022
T12 (p.u.)	0.9	1.1	0.9027	0.907	0.9022	0.9802	0.9413	0.903	0.9217
T15 (p.u.)	0.9	1.1	0.9496	0.9542	0.9687	0.9844	0.9749	1.0967	0.981
T36 (p.u.)	0.9	1.1	0.9454	0.9497	0.9634	0.983	0.981	0.9207	0.9726
QC10 (MVAr)	0	5	4.986	5	4.501	4.05	4.986	4.7	0.37
QC12 (MVAr)	0	5	4.927	4.69	1.691	0.64	4.856	1.63	0.04
QC15 (MVAr)	0	5	5	4.72	4.268	4.84	4.549	4.86	1.21
QC17 (MVAr)	0	5	4.881	4.68	0.38	1.91	4.988	4.17	0.06
QC20 (MVAr)	0	5	4.648	4.02	4.918	4.49	4.983	4.91	3.87
QC21 (MVAr)	0	5	4.986	4.9	4.33	4.74	4.776	4.56	3.49
QC23 (MVAr)	0	5	4.114	2.55	4.869	3.63	4.996	4.61	1.45
QC24 (MVAr)	0	5	4.95	4.94	4.89	2.87	4.835	4.66	4.91
QC29 (MVAr)	0	5	2.146	2.48	1.509	2.53	4.766	2.5	4.11
APL (MW)			**4.5086**	**4.1811**	5.7777	5.4911	4.7272	5.9401	**5.49**
AVD (p.u.)			2.3375	2.0303	**0.0879**	**0.0861**	2.082	1.6576	**0.1118**
VSI (p.u.)			0.1119	0.1257	0.1371	0.1384	**0.1132**	**0.1107**	0.142
QG1 (MVAr)	− 20	150	NA	−0.35	NA	−18.39	NA	−13.73	16.25
QG2 (MVAr)	− 20	60	NA	11.53	NA	−19.5	NA	−14.81	−6.94
QG5 (MVAr)	− 15	62.5	NA	24.28	NA	57.27	NA	14.61	60.83
QG8 (MVAr)	− 15	48.7	NA	24.52	NA	34.94	NA	29.97	−5.44
QG11 (MVAr)	− 10	40	NA	6.1	NA	8.01	NA	6.83	11.08
QG13 (MVAr)	− 15	44.7	NA	−3.13	NA	−7.72	NA	−14.08	5.35
CPU time (s)			128.75	126.78	130.33	129.99	127.13	126.87	126.07

Bold values are signifying the optimal results of single and multi-objective functions for different cases of the proposed work

OFs-which are multi-objective minimization of combined APL and AVD and single-objective minimization of APL, AVD, and VSI-are obtained. The optimization technique is executed 25 times to cover all the established scenarios in the current study, which consists of 25 situations, allowing a complete investigation of each instance.

Table 9 shows the minimal APL (corresponding to case 9), minimal AVD (corresponding to case 10) and minimum VSI (corresponding to case 11) for each generated scenario in Table 7. From these likely computed APL, AVD, and VSI for each scenario, an expected APL (EAPL) (for case 9), an expected AVD (EAVD) (for case 10), and an expected VSI (EVSI) (for case 11) are computed and reported in Table 9. Here's how these computations are carried out:

$$EAPL = \sum_{i=1}^{N_{ec}} \rho_i \times APL_i \tag{34}$$

$$EAVD = \sum_{i=1}^{N_{ec}} \rho_i \times AVD_i \tag{35}$$

$$EVSI = \sum_{i=1}^{N_{ec}} \rho_i \times VSI_i \tag{36}$$

where: i indicates scenario index; N_{ec} is the number of scenario; ρ_i indicates probability of i^{th} scenario.

Table 9 is produced in order to show the results of case 12, where the goal is to simultaneously minimize the APL and the AVD for 25 situations of Table 7.

Table 6 Simulation results of case studies with fixed loading (100%) for the adapted IEEE 30 bus system incorporating SVC

Control parameters	Min.	Max.	Case 5 [MMKE]	Case 6 [MMKE]	Case 7 [MMKE]	Case 8 [MMKE]	Case 8a [MMKE]
V1 (p.u.)	0.95	1.1	1.0991	1.0184	1.055	1.0235	1.037
V2 (p.u.)	0.95	1.1	1.0925	1.0156	1.0461	1.0186	1.0341
V5 (p.u.)	0.95	1.1	1.0718	1.0213	1.0279	1.013	1.0108
V8 (p.u.)	0.95	1.1	1.0753	0.9877	1.0499	0.9974	0.9896
V11 (p.u.)	0.95	1.1	1.0977	1.0331	1.0895	1.0506	1.0502
V13 (p.u.)	0.95	1.1	1.0997	1.0028	1.0149	1.014	1.0034
T11 (p.u.)	0.9	1.1	1.0465	1.0349	1.0589	1.051	1.0369
T12 (p.u.)	0.9	1.1	0.9044	0.9623	0.9008	0.9405	0.9279
T15 (p.u.)	0.9	1.1	0.9779	1.0027	1.0967	0.9903	0.9753
T36 (p.u.)	0.9	1.1	0.9715	0.9891	0.9177	0.9533	0.9544
QC10 (MVAr)	0	5	4.91	0.68	4.76	1.34	5
QC12 (MVAr)	0	5	4.98	0.02	1.63	0.14	1.97
QC15 (MVAr)	0	5	4.87	4.61	4.86	2.08	4.5
QC17 (MVAr)	0	5	4.86	2.38	4.49	0.76	0.09
QC20 (MVAr)	0	5	4.23	4.89	4.43	3.78	4.97
QC21 (MVAr)	0	5	4.95	4.66	4.56	2.49	4.93
QC23 (MVAr)	0	5	2.72	1.87	4.73	1.85	4.96
QC24 (MVAr)	0	5	4.98	4.56	4.92	4.51	4.95
QC29 (MVAr)	0	5	2.49	1.91	2.5	0.38	1.75
Optimal location of SVC1			21	21	21	21	21
Optimal location of SVC2			24	24	24	24	24
QSVC1 (MVAr)	− 10	10	9.9352	9.7651	9.8764	9.9765	9.897
QSVC2 (MVAr)	− 10	10	9.5125	9.5431	9.5007	9.5761	8.9978
APL (MW)			**4.1001**	5.2801	6.0102	**4.9305**	**5.05**
AVD (p.u.)			1.9928	**0.0739**	1.7765	**0.1025**	**0.1208**
VSI (p.u.)			0.1268	0.1391	**0.1097**	0.1413	**0.1385**
QG1 (MVAr)	− 20	150	−8.59	−17.07	−14.56	−12.46	−10.3
QG2 (MVAr)	− 20	60	10.4	6.63	−19.5	7.67	39.54
QG5 (MVAr)	− 15	62.5	24.46	54.43	17.67	41.9	32.95
QG8 (MVAr)	− 15	48.7	24.9	0.65	28.72	16.87	2.9
QG11 (MVAr)	− 10	40	11.35	16.52	14.24	24.39	22.53
QG13 (MVAr)	− 15	44.7	0.23	0.74	−14.99	4.04	−3.56
CPU Time (s)			125.55	129.02	126.09	125.65	125.76

Bold values are signifying the optimal results of single and multi-objective functions for different cases of the proposed work

The test setup with SVC is used for the experiments for cases 13-16, and the same circumstances as in Table 11 are used. Scenario-based experimental results for cases 13-15 are presented in Table 11, while results for case 16 are presented in Table 12.

When MMKE is applied to test systems with and without SVC, the following points are observed:

- EAPL was 2.6521 MW (case 9) without SVC, but with SVC, it drops to 2.5101 MW (case 13).
- The EAVD in example 10 was 0.0628 p.u. without SVC; in case 14, it decreases to 0.0595 p.u. with SVC.
- The EVSI in case 11 was 0.0856 p.u. without SVC; in case 14, the EVSI decreases to 0.0796 p.u. with SVC incorporated.
- Observing cases-12 and-16 simultaneously reveals that connecting SVC (in case-16) reduces EAPL and EAVD by 0.141 MW and 0.0044 p.u., respectively, compared to case-12 (*i.e.* without SVC).

These observations suggest that reducing APL, AVD, and VSI individually as well as collectively reducing APL and AVD, use of SVC devices improve the performances of the power network's operations.

Table 7 The generated scenarios of load demand, SI, WS and TFR with their corresponding probabilities

Scenario No.	%Loading	Wind farm$_1$ at bus 5 W(m/s)	Solar PV at bus 11 SI (W/m^2)	Wind Farm$_2$ and tidal power at bus 13 WS (m/s)	TFR (m^3/s)	Scenario probability
1	85.4998	15.5643	454.2837	16.7654	130.8877	0.005
2	93.0663	4.9876	783.4354	7.6512	120.5432	0.001
3	84.2514	8.9876	897.8735	2.7809	135.6644	0.004
4	76.5664	3.6543	305.5632	15.8765	116.5432	0.003
5	80.3714	7.6543	289.6734	11.9876	162.0987	0.004
6	98.3753	11.8765	1055.3243	24.7654	157.4321	0.005
7	87.0929	17.5412	987.7676	23.8765	118.3421	0.001
8	88.9426	19.2098	89.7655	0.5323	153.5432	0.04
9	92.3917	6.9861	0	1.003	156.3342	0.011
10	110.5316	17.8702	107.6754	3.7865	148.6565	0.005
11	81.5345	13.731	755.8765	6.1122	118.6543	0.001
12	76.5164	13.7654	201.3321	6.9832	178.7687	0.081
13	92.7455	7.8965	95.8908	13.345	114.7765	0.009
14	77.6634	12.8743	1004.5634	14.4321	164.5434	0.002
15	71.8947	15.8667	432.4454	12.865	125.4409	0.001
16	106.8372	3.8751	212.7609	0.9876	155.8976	0.076
17	68.1133	17.6757	454.5645	3.872	138.6543	0.3
18	74.0076	12.5436	390.8981	8.3241	169.3342	0.049
19	97.2919	11.8043	107.9891	6.3421	160.1213	0.001
20	71.5136	6.765	0	4.4531	131.3423	0.211
21	100.2235	4.6754	234.8976	17.4532	50.098	0.077
22	86.3776	7.2342	243.0098	2.9861	167.6548	0.046
23	78.5634	9.7653	465.9878	6.2324	136.3377	0.05
24	78.5748	12.541	777.9872	14.321	110.9899	0.001
25	84.8562	3.6755	867.1102	6.876	127.6544	0.016

Table 8 Selected scenarios, load demand and corresponding output powers of solar, both wind farms, tidal power unit and probabilities

Scenario No.	%Loading	Wind farm$_1$ at bus 5 WP1 (MW)	Solar PV at bus 11 SI PV power (MW)	Wind farm$_2$ at bus 13 WP2 (MW)	Tidal power at bus 13 tidal power (MW)	Wind Farm$_2$ + tidal power at bus 13 tidal power + WP2 (MW)	Scenario probability
1	85.4998	72.4863	22.7142	45	3.5798	48.5798	0.005
2	93.0663	11.4669	39.1718	16.1003	3.2969	19.3972	0.001
3	84.2514	34.5438	44.8937	0	3.7105	3.7105	0.004
4	76.5664	3.7748	15.2782	44.5725	3.1875	47.76	0.003
5	80.3714	26.8517	14.4837	31.1109	4.4334	35.5444	0.004
6	98.3753	51.2106	50	45	4.3058	49.3058	0.005
7	87.0929	75	49.3884	45	3.2367	48.2367	0.001
8	88.9426	75	3.3574	0	4.1994	4.1994	0.04
9	92.3917	22.9967	0	0	4.2758	4.2758	0.011
10	110.5316	75	4.8308	2.7225	4.0658	6.7883	0.005
11	81.5345	61.9096	37.7938	10.773	3.2452	14.0182	0.001
12	76.5164	62.1081	10.0666	13.788	4.8894	18.6774	0.081
13	92.7455	28.249	3.8313	35.8096	3.1392	38.9488	0.009
14	77.6634	56.9671	50	39.5727	4.5003	44.073	0.002
15	71.8947	74.231	21.6223	34.1481	3.4308	37.5789	0.001
16	106.8372	5.0487	10.638	0	4.2638	4.2638	0.076
17	68.1133	75	22.7282	3.0185	3.7922	6.8107	0.3
18	74.0076	55.0592	19.5449	18.4296	4.6313	23.0609	0.049
19	97.2919	50.794	4.859	11.5688	4.3794	15.9482	0.001
20	71.5136	21.7212	0	5.03	3.5922	8.6222	0.211
21	100.2235	9.6658	11.7449	45	1.3702	46.3702	0.077
22	86.3776	24.4281	12.1505	0	4.5854	4.5854	0.046
23	78.5634	39.0306	23.2994	11.1891	3.7289	14.918	0.05
24	78.5748	55.0442	38.8994	39.1881	3.0356	42.2237	0.001
25	84.8562	3.8971	43.3555	13.4169	3.4914	16.9083	0.016

Table 9 Single-objective ORPD evaluated cases with time-varying demand and uncertain renewable power

Scenario No.	%Loading	Wind farm$_1$ at bus 5	Solar PV at bus 11	Wind farm$_2$ at bus 13	Tidal power at bus 13	Wind farm$_2$ + tidal at bus 13	Scenario probability	Scenario-based APL	Scenario-based AVD	Scenario-based VSI
		WP_1 (MW)	PV (MW)	WP_2 (MW)	HP (MW)	$HP+WP_2$ (MW)	Δsc	(MW)	(p.u.)	(p.u.)
1	85.4998	72.4863	22.7142	45	3.5798	48.5798	0.005	1.9987	0.0721	0.0923
2	93.0663	11.4669	39.1718	16.1003	3.2969	19.3972	0.001	2.2234	0.0652	0.0987
3	84.2514	34.5438	44.8937	0	3.7105	3.7105	0.004	2.5623	0.0792	0.0875
4	76.5664	3.7748	15.2782	44.5725	3.1875	47.76	0.003	2.8972	0.07021	0.0917
5	80.3714	26.8517	14.4837	31.1109	4.4334	35.5444	0.004	2.0911	0.0756	0.0884
6	98.3753	51.2106	50	45	4.3058	49.3058	0.005	1.7654	0.0436	0.0812
7	87.0929	75	49.3884	45	3.2367	48.2367	0.001	2.0987	0.0711	0.0798
8	88.9426	75	3.3574	0	4.1994	4.1994	0.04	1.8976	0.0528	0.0901
9	92.3917	22.9967	0	0	4.2758	4.2758	0.011	2.1231	0.0712	0.0786
10	110.5316	75	4.8308	2.7225	4.0658	6.7883	0.005	3.7865	0.0727	0.0854
11	81.5345	61.9096	37.7938	10.773	3.2452	14.0182	0.001	1.7654	0.0648	0.0965
12	76.5164	62.1081	10.0666	13.788	4.8894	18.6774	0.081	1.6754	0.0562	0.0876
13	92.7455	28.249	3.8313	35.8096	3.1392	38.9488	0.009	3.3241	0.0726	0.0811
14	77.6634	56.9671	50	39.5727	4.5003	44.073	0.002	3.3141	0.0781	0.0912
15	71.8947	74.231	21.6223	34.1481	3.4308	37.5789	0.001	4.0967	0.0744	0.0765
16	106.8372	5.0487	10.638	0	4.2638	4.2638	0.076	3.1211	0.0704	0.0729
17	68.1133	75	22.7282	3.0185	3.7922	6.8107	0.3	1.7654	0.0543	0.0897
18	74.0076	55.0592	19.5449	18.4296	4.6313	23.0609	0.049	1.4325	0.0676	0.0786
19	97.2919	50.794	4.859	11.5688	4.3794	15.9482	0.001	4.0982	0.0675	0.0872
20	71.5136	21.7212	0	5.03	3.5922	8.6222	0.211	4.6334	0.0701	0.0876
21	100.2235	9.6658	11.7449	45	1.3702	46.3702	0.077	3.4477	0.0643	0.0765
22	86.3776	24.4281	12.1505	0	4.5854	4.5854	0.046	2.7865	0.0763	0.0861
23	78.5634	39.0306	23.2994	11.1891	3.7289	14.918	0.05	1.3392	0.0603	0.0891
24	78.5748	55.0442	38.8994	39.1881	3.0356	42.2237	0.001	1.2906	0.0486	0.0817
25	84.8562	3.8971	43.3555	13.4169	3.4914	16.9083	0.016	1.5432	0.0751	0.0766
							Case9: EAPL= $\sum \Delta sc \times$ **APL=2.6521**			
							Case10: EAVD= $\sum \Delta sc \times$ **AVD= 0.0628**			
							Case11: EVSI= $\sum \Delta sc \times$ **VSI= 0.0856**			

Bold values are signifying the optimal results of single and multi-objective functions for different cases of the proposed work

In case 10 under uncertainty scenarios 10 and 15, where SVC is not introduced with test network, the voltage deviations at various load buses are shown in Fig. 8. Voltage variations over different load buses for case 14 (*i.e.*, test set up with SVC) under identical uncertainty situations are displayed in Fig. 9. Only two of the twenty-five scenarios-scenarios 10 and 15-are selected to display the VD profile over load buses since it is not feasible to display the VD profile for every scenario. Moreover, scenarios 10 and 15 illustrate overloaded and under-loaded situations, respectively. The improvement of the VD profile after SVC has been applied with the test systems may be investigated by closely examining Figs. 8, 9 concurrently.

5.3 Friedman test

To verify the performance of MMKE over other evolutionary algorithms (EA) (like: Biogeography-based optimization (BBO), modified artificial hummingbird algorithm, given in [6]), Friedman test has been conducted over the obtained results from various EAs. The results are shown in Table 13

A nonparametric version of the one-way repeated measures test, the Friedman test is an extension of the Wilcoxon signed-rank test. The null hypothesis, according to Friedman, is that all k related variables are produced by the same population. k is three here. The k variables are rated from 1 to k for every case. These ranks form the basis of the test statistic. Table 15 shows the computed ranks for Friedman Test.

Table 10 Multi-objective ORPD evaluated cases with time-varying demand and uncertain renewable power

Scenario No.	%Loading	Wind farm$_1$ at bus 5	Solar PV at bus 11	Wind farm$_2$ at bus 13	Tidal power at bus 13	Wind farm$_2$ + Tidal at bus 13	Scenario probability	Scenario-based APL	Scenario-based AVD	Objective value LVD (Case 12) $\lambda_l \cdot \text{APL} + \lambda_{vd} \cdot \text{AVD}$
		WP_1 (MW)	PV (MW)	WP_2 (MW)	HP (MW)	(MW)	Δsc	(MW)	(p.u.)	
1	85.4998	72.4863	22.7142	45	3.5798	48.5798	0.005	2.6875	0.0763	3.4505
2	93.0663	11.4669	39.1718	16.1003	3.2969	19.3972	0.001	3.1422	0.0853	3.9952
3	84.2514	34.5438	44.8937	0	3.7105	3.7105	0.004	2.9878	0.0871	3.8588
4	76.5664	3.7748	15.2782	44.5725	3.1875	47.76	0.003	4.2345	0.0872	5.1065
5	80.3714	26.8517	14.4837	31.1109	4.4334	35.5444	0.004	3.0011	0.0798	3.7991
6	98.3753	51.2106	50	45	4.3058	49.3058	0.005	2.8752	0.0673	3.5482
7	87.0929	75	49.3884	45	3.2367	48.2367	0.001	2.5563	0.0787	3.3433
8	88.9426	75	3.3574	0	4.1994	4.1994	0.04	2.4372	0.0676	3.1132
9	92.3917	22.9967	0	0	4.2758	4.2758	0.011	3.1092	0.0799	3.9082
10	110.5316	75	4.8308	2.7225	4.0658	6.7883	0.005	4.4536	0.0845	5.2986
11	81.5345	61.9096	37.7938	10.773	3.2452	14.0182	0.001	2.1652	0.0876	3.0412
12	76.5164	62.1081	10.0666	13.788	4.8894	18.6774	0.081	2.2263	0.0734	2.9603
13	92.7455	28.249	3.8313	35.8096	3.1392	38.9488	0.009	3.5624	0.0788	4.3504
14	77.6634	56.9671	50	39.5727	4.5003	44.073	0.002	4.5234	0.0746	5.2694
15	71.8947	74.231	21.6223	34.1481	3.4308	37.5789	0.001	4.5541	0.0832	5.3861
16	106.8372	5.0487	10.638	0	4.2638	4.2638	0.076	3.9992	0.0753	4.7522
17	68.1133	75	22.7282	3.0185	3.7922	6.8107	0.3	2.9225	0.0675	3.5975
18	74.0076	55.0592	19.5449	18.4296	4.6313	23.0609	0.049	3.4243	0.0776	4.2003
19	97.2919	50.794	4.859	11.5688	4.3794	15.9482	0.001	4.7721	0.0698	5.4701
20	71.5136	21.7212	0	5.03	3.5922	8.6222	0.211	4.1014	0.0803	4.9044
21	100.2235	9.6658	11.7449	45	1.3702	46.3702	0.077	3.6732	0.0765	4.4382
22	86.3776	24.4281	12.1505	0	4.5854	4.5854	0.046	2.9871	0.0834	3.8211
23	78.5634	39.0306	23.2994	11.1891	3.7289	14.918	0.05	2.8721	0.0707	3.5791
24	78.5748	55.0442	38.8994	39.1881	3.0356	42.2237	0.001	3.6735	0.0728	4.4015
25	84.8562	3.8971	43.3555	13.4169	3.4914	16.9083	0.016	2.2345	0.0801	3.0355
					Case 12: EAPL= $\sum \Delta_{sc} \times$ **APL= 3.2742** $\lambda_l = 1, \lambda_{vd} = 10$					
					EAVD= $\sum \Delta_{sc} \times$ **AVD= 0.0742**					

Bold values are signifying the optimal results of single and multi-objective functions for different cases of the proposed work

Table 11 Single-objective ORPD evaluated cases with time-varying demand and uncertain renewable power with SVC

Scenario No.	%Loading	Wind farm$_1$ at bus 5 WP_1 (MW)	Solar PV at bus 11 PV (MW)	Wind farm$_2$ at bus 13 WP_2 (MW)	Tidal power at bus 13 P_{Tidal} (MW)	Wind Farm$_2$ + Tidal at bus 13 HP+WP_2 (MW)	Scenario probability Δsc	Scenario-based APL (MW)	Scenario- based AVD (p.u.)	Scenario -based VSI (p.u.)
1	85.4998	72.4863	22.7142	45	3.5798	48.5798	0.005	2.4561	0.0702	0.0787
2	93.0663	11.4669	39.1718	16.1003	3.2969	19.3972	0.001	2.6767	0.0564	0.0802
3	84.2514	34.5438	44.8937	0	3.7105	3.7105	0.004	2.2341	0.0756	0.0767
4	76.5664	3.7748	15.2782	44.5725	3.1875	47.76	0.003	2.1558	0.0544	0.0812
5	80.3714	26.8517	14.4837	31.1109	4.4334	35.5444	0.004	1.8756	0.0654	0.0809
6	98.3753	51.2106	50	45	4.3058	49.3058	0.005	1.2345	0.0332	0.0787
7	87.0929	75	49.3884	45	3.2367	48.2367	0.001	2.7864	0.0687	0.0822
8	88.9426	75	3.3574	0	4.1994	4.1994	0.04	2.3332	0.0476	0.0876
9	92.3917	22.9967	0	0	4.2758	4.2758	0.011	2.0043	0.0689	0.0745
10	110.5316	75	4.8308	2.7225	4.0658	6.7883	0.005	1.7659	0.0711	0.0824
11	81.5345	61.9096	37.7938	10.773	3.2452	14.0182	0.001	1.1122	0.0623	0.0836
12	76.5164	62.1081	10.0666	13.788	4.8894	18.6774	0.081	1.1067	0.0534	0.0833
13	92.7455	28.249	3.8313	35.8096	3.1392	38.9488	0.009	3.3429	0.0712	0.0673
14	77.6634	56.9671	50	39.5727	4.5003	44.073	0.002	3.6352	0.0696	0.0754
15	71.8947	74.231	21.6223	34.1481	3.4308	37.5789	0.001	2.8745	0.0706	0.0709
16	106.8372	5.0487	10.638	0	4.2638	4.2638	0.076	3.3421	0.0678	0.0701
17	68.1133	75	22.7282	3.0185	3.7922	6.8107	0.3	2.7864	0.0505	0.0854
18	74.0076	55.0592	19.5449	18.4296	4.6313	23.0609	0.049	1.9421	0.0624	0.0734
19	97.2919	50.794	4.859	11.5688	4.3794	15.9482	0.001	3.3344	0.0655	0.0876
20	71.5136	21.7212	0	5.03	3.5922	8.6222	0.211	2.4987	0.0677	0.0736
21	100.2235	9.6658	11.7449	45	1.3702	46.3702	0.077	3.3987	0.0621	0.0721
22	86.3776	24.4281	12.1505	0	4.5854	4.5854	0.046	2.4538	0.0745	0.0855
23	78.5634	39.0306	23.2994	11.1891	3.7289	14.918	0.05	1.5632	0.0573	0.0885
24	78.5748	55.0442	38.8994	39.1881	3.0356	42.2237	0.001	1.9825	0.0675	0.0808
25	84.8562	3.8971	43.3555	13.4169	3.4914	16.9083	0.016	2.3561	0.0653	0.0798
					Case 13: EAPL= $\sum \Delta_{sc} \times$ APL= 2.5101					
					Case14: EAVD= $\sum \Delta_{sc} \times$ AVD= 0.0595					
					Case15: EVSI= $\sum \Delta_{sc} \times$ VSI= 0.0796					

Bold values are signifying the optimal results of single and multi-objective functions for different cases of the proposed work

Table 12 Multi-objective ORPD evaluted cases with time-varying demand and uncertain renewable power with SVC

Scenario No.	%Loading	Wind farm$_1$ at bus 5	Solar PV at bus 11	Wind farm$_2$ at bus 13	Tidal power at bus 13	Wind farm$_2$ + Tidal at bus 13 HP+WP$_2$	Scenario probability	Scenario-based APL	Scenario-based AVD	Objective value LVD (Case 16) λ_l·APL+λ_{vd}·AVD
		WP$_1$ (MW)	PV (MW)	WP$_2$ (MW)	P_{Tidal} (MW)	(MW)	Δsc	(MW)	(p.u.)	
1	85.4998	72.4863	22.7142	45	3.5798	48.5798	0.005	2.4531	0.0747	3.2001
2	93.0663	11.4669	39.1718	16.1003	3.2969	19.3972	0.001	2.8765	0.0713	3.5895
3	84.2514	34.5438	44.8937	0	3.7105	3.7105	0.004	3.1211	0.0712	3.8331
4	76.5664	3.7748	15.2782	44.5725	3.1875	47.76	0.003	2.1109	0.0701	2.8119
5	80.3714	26.8517	14.4837	31.1109	4.4334	35.5444	0.004	2.4321	0.0701	3.1331
6	98.3753	51.2106	50	45	4.3058	49.3058	0.005	2.4434	0.0722	3.1654
7	87.0929	75	49.3884	45	3.2367	48.2367	0.001	2.2212	0.0644	2.8652
8	88.9426	75	3.3574	0	4.1994	4.1994	0.04	2.3342	0.0622	2.9562
9	92.3917	22.9967	0	0	4.2758	4.2758	0.011	2.9984	0.0755	3.7534
10	110.5316	75	4.8308	2.7225	4.0658	6.7883	0.005	3.5653	0.0765	4.3303
11	81.5345	61.9096	37.7938	10.773	3.2452	14.0182	0.001	2.9875	0.0732	3.7195
12	76.5164	62.1081	10.0666	13.788	4.8894	18.6774	0.081	2.1103	0.0643	2.7533
13	92.7455	28.249	3.8313	35.8096	3.1392	38.9488	0.009	3.6759	0.0732	4.4079
14	77.6634	56.9671	50	39.5727	4.5003	44.073	0.002	3.2344	0.0612	3.8464
15	71.8947	74.231	21.6223	34.1481	3.4308	37.5789	0.001	2.1441	0.0602	2.7461
16	106.8372	5.0487	10.638	0	4.2638	4.2638	0.076	3.0672	0.0765	3.8322
17	68.1133	75	22.7282	3.0185	3.7922	6.8107	0.3	3.7675	0.0643	4.4105
18	74.0076	55.0592	19.5449	18.4296	4.6313	23.0609	0.049	2.3243	0.0723	3.0473
19	97.2919	50.794	4.859	11.5688	4.3794	15.9482	0.001	3.4421	0.0624	4.0661
20	71.5136	21.7212	0	5.03	3.5922	8.6222	0.211	3.0514	0.0756	3.8074
21	100.2235	9.6658	11.7449	45	1.3702	46.3702	0.077	3.7657	0.0722	4.4877
22	86.3776	24.4281	12.1505	0	4.5854	4.5854	0.046	2.7771	0.0745	3.5221
23	78.5634	39.0306	23.2994	11.1891	3.7289	14.918	0.05	2.4587	0.0687	3.1457
24	78.5748	55.0442	38.8994	39.1881	3.0356	42.2237	0.001	2.2131	0.0664	2.8771
25	84.8562	3.8971	43.3555	13.4169	3.4914	16.9083	0.016	2.9915	0.0764	3.7555
						Case 16: EAPL= $\sum \Delta_{sc} \times$ APL= 3.1332 λ_l=1, λ_{vd}=10				
						EAVD= $\sum \Delta_{sc} \times$ AVD = 0.0698				

Bold values are signifying the optimal results of single and multi-objective functions for different cases of the proposed work

Table 13 Comparative study of different optimizations of ORPD with time-varying demand for the IEEE 30-bus system

Case	Objectives	MMKE	BBO	MAHA [6]	AHA [6]	GWO [6]	SCA [6]	BWO [6]
Case 1	APL (MW)	4.1811	4.3251	4.5086	4.5276	4.5470	4.7953	4.7831
Case 2	AVD (p.u.)	0.0861	0.0872	0.0879	0.0919	0.1308	0.1845	0.1241
Case 3	L-index	0.1107	0.1122	0.1132	–	–	–	–

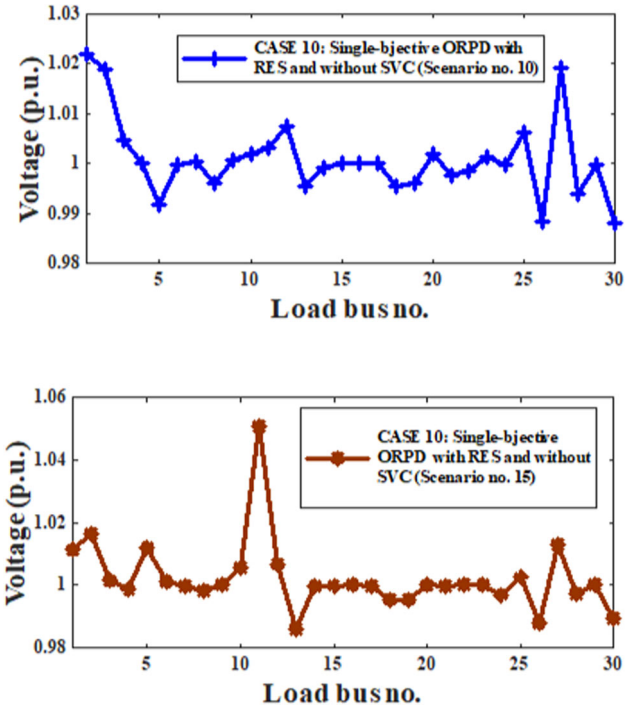

Fig. 8 Load bus voltage deviations for case-10 for uncertainty scenarios 10 and 15

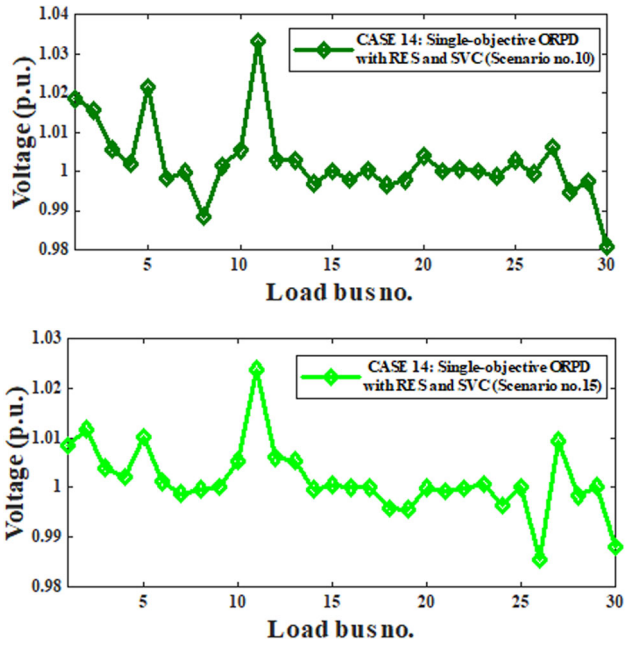

Fig. 9 Load bus voltage fluctuations for case-14 for uncertainty scenarios 10 and 15

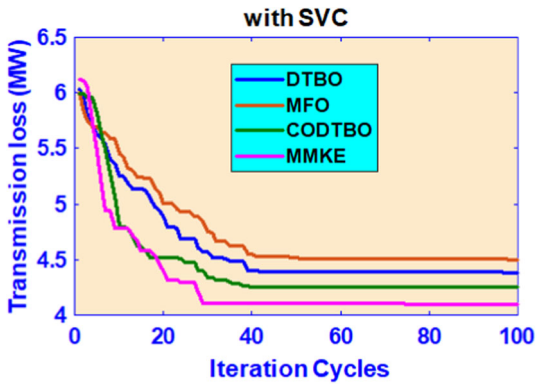

Fig. 10 Convergence characteristics of APL minimization problem using DTBO, MFO, CODTBO and MMKE having SVC with test network

Table 14 Statistical analysis on ORPD problem with SVC

Algorithms	Active power loss (MW)			
	Best	Average	Worst	(sec)
MMKE	4.1001	4.3304	4.7254	125.53
CODTBO [53]	4.2504	4.4732	4.8732	135.42
DTBO [53]	4.3872	4.6731	4.9599	141.23
MFO [54]	4.5035	4.8463	5.1234	144.32

Here expected Rank E(R) is 6, χ^2 value is 6 and degree of freedom (DF) is 2. From chi-square distribution table, the critical chi-square value is obtained as 5.99 for DF 2 and significance level 0.05. Calculated chi-square is 6 which is greater than critical chi-square 5.99 that means null hypothesis is rejected. It implies that there is a significant difference at the outcomes obtained by the EAs. It establishes the superior performance of MMKE over other EAs.

5.4 3rd Module

In order to examine how well MMKE performs on extremely complicated networks, the 3rd Module of study is being conducted. Therefore, in this module IEEE 118 bus network has been chosen as test network which is summarized in Table 16. From Table 4, it is found that in this test system, Case 17–19 are being conducted without considering SVC with the test system and Case 20 to 22 are being carried out where SVC has been considered with the specified test system. The simulation results for Case 17–19 where SVC is not

Table 15 Friedman test ranks

Case	Objectives	MMKE	BBO	MAHA [6]
Case 1	APL(MW)	4.1811−rank 3	4.3251−rank 2	4.5086−rank 1
Case 2	AVD($p.u.$)	0.0861−rank 3	0.0872−rank 2	0.0879−rank 1
Case 3	L−index	0.1107−rank 3	0.1122−rank 2	0.1132−rank 1
	∑Rank	9	6	3

incorporated with the system are presented in Table 17 and the outcomes for Case 20–22 where SVC has been included with specified system are given in Table 18. Figure 11 provides the voltage deviations over different buses for Case 18 and Case 21. Simulation results clearly suggest the efficacy of the proposed algorithms for various objective functions of large scale power system.

6 Conclusions

In the present work, MMKE has been used to address the ORPD problem over three test settings, which are demonstrated in three study modules. An IEEE 30 bus configuration is chosen as traditional network in the first module, and RESs are connected to the traditional network in the second module. Finally conventional IEEE 118 bus has been considered in module three of the current study. In order to address the stochastic of load demand and RESs, the study's intermediate phase uses a scenario generation and reduction approach, whereas its earlier phases and the concluding phase are conducted in a deterministic context. The significant outcomes of the proposed work are outlined in the following aspects.

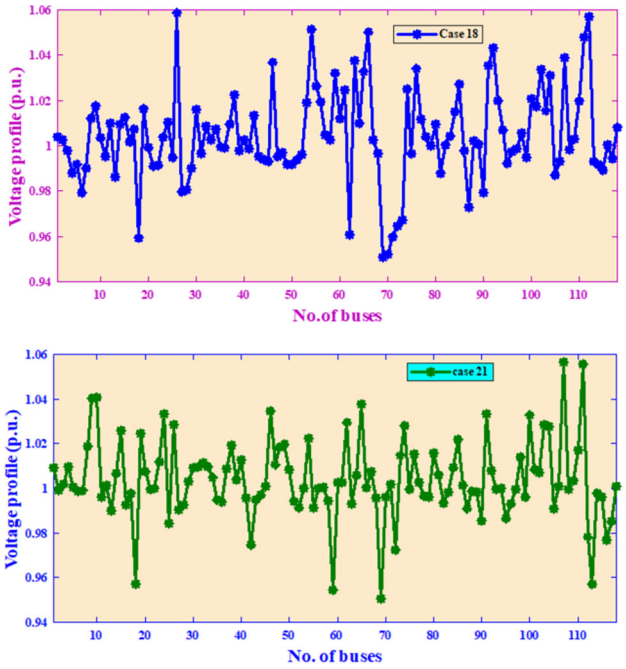

Fig. 11 Load bus voltage fluctuations for Case-18 and Case 21 under fixed loading

Table 16 An overview of IEEE 118- bus system under study

Item	Quantity	Details
Buses	118	[55]
Branches	186	[55]
Thermal generators	54	Buses: 69 (swing), 1, 4, 6, 8, 10, 12, 15, 18, 19, 24, 25, 26, 27, 31, 32, 34, 36, 40, 42, 46, 49, 54, 55, 56, 59, 61, 62, 65, 66, 69, 70, 72, 73, 74, 76, 77, 80, 85, 87, 89, 90, 91, 92, 99, 100, 103, 104, 105, 107, 110, 111, 112, 113 and 116
Tap changing transformer	9	Branches: (8–5), (26–35),(30–17),(38–37),(63–59),(64–61),(65–66),(68–69) and (81–80)
Control variables	77	voltages (54) + transformer tap settings (9) + shunt capacitor (14)
Load demand		4242.0 MW, 1439.0 MVAr
Range of load bus voltage	64	[0.95−1.05] p.u.
SVC	2	Branch location and rating optimized
Compensation devices	14	Buses: 5, 34, 37, 44, 45, 46, 48, 74, 79, 82, 83, 105, 107 and 110

- Three proposed systems, namely ORPD, ORPD with RESs (wind, solar, tidal) and ORPD with RESs and FACTS devices are effectively analysed by the novel MMKE technique.
- Optimal solution on single- and multi-objective functions to minimize APL, AVD, and VSI are successfully analysed using MMKE approach.
- Initially, a comparive study of MMKE with BBO, MAHA, GWO and SCA has been made for ORPD problem on IEEE 30-bus system for optimal solution of APL, AVD and L-index. The obtained APL using MMKE is found to be 4.1811 Mw which is 3.4%, 7.8%, 8.8% and 14% better than BBO, MAHA, GWO and SCA optimizations. Additionally, AVD and L-index achieved using MMKE are 0.0861 p.u and 0.1107, respectively, which are preferable than the other algorithms. The result exhibits significantly better performance of MMKE than the existing optimization techniques.
- The statistical analysis made on ORPD with FACTS devices for IEEE 30 bus system shows that the obtained best, mean and worst results are very closed than those obtained by the state-of-the-art methods. This signifies the robustness of proposed approach.

Table 17 Simulation results of case studies with fixed loading (100%) for the IEEE 118-bus system (without SVC)

Control parameters	Min.	Max.	Case 17	Case 18	19	Control parameters	Min.	Max.	Case 17	Case 18	19
V1 (p.u.)	0.94	1.06	0.9637	1.0114	0.9824	V91 (p.u.)	0.94	1.06	1.0032	1.059	0.998
V4 (p.u.)	0.94	1.06	0.983	0.9949	0.9985	V92 (p.u.)	0.94	1.06	1.0237	1.0212	1.0237
V6 (p.u.)	0.94	1.06	0.9632	0.9792	0.9477	V99 (p.u.)	0.94	1.06	1.0228	0.9949	1.022
V8 (p.u.)	0.94	1.06	1.028	0.9973	0.971	V100 (p.u.)	0.94	1.06	1.0186	1.0209	1.0263
V10 (p.u.)	0.94	1.06	1.0581	1.0037	1.0424	V103 (p.u.)	0.94	1.06	1.0174	1.0267	0.9974
V12 (p.u.)	0.94	1.06	0.9635	1.0148	0.993	V104 (p.u.)	0.94	1.06	1.0063	1.0089	0.9982
V15 (p.u.)	0.94	1.06	0.9721	0.9956	0.9742	V105 (p.u.)	0.94	1.06	1.007	0.9866	1.0399
V18 (p.u.)	0.94	1.06	0.9827	0.9593	1.0109	V107 (p.u.)	0.94	1.06	1.0071	1.0389	1.0267
V19 (p.u.)	0.94	1.06	0.9753	1.0326	1.0446	V110 (p.u.)	0.94	1.06	1.0126	1.0197	0.9767
V24 (p.u.)	0.94	1.06	1.0232	0.9965	1.0191	V111 (p.u.)	0.94	1.06	1.0209	1.0479	0.9742
V25 (p.u.)	0.94	1.06	1.0339	0.995	1.013	V112 (p.u.)	0.94	1.06	0.9944	1.0313	1.0485
V26 (p.u.)	0.94	1.06	1.0539	0.9497	1.0237	V113 (p.u.)	0.94	1.06	1.0038	1.0071	0.9492
V27 (p.u.)	0.94	1.06	1.0131	1.0088	1.0221	V116 (p.u.)	0.94	1.06	1.011	0.9844	0.9642
V31 (p.u.)	0.94	1.06	1.001	0.9966	1.0592	T8 (p.u.)	0.9	1.1	0.9985	0.9913	1.0385
V32 (p.u.)	0.94	1.06	1.0075	1.0058	1.0094	T32 (p.u.)	0.9	1.1	1.0496	1.0245	0.9966
V34 (p.u.)	0.94	1.06	1.034	1	1.0586	T36 (p.u.)	0.9	1.1	1.0371	1.0405	1.0521
V36 (p.u.)	0.94	1.06	1.0295	0.999	0.9976	T51 (p.u.)	0.9	1.1	1.0086	0.9793	0.9372
V40 (p.u.)	0.94	1.06	1.0109	0.9948	0.9909	T93 (p.u.)	0.9	1.1	1.042	0.9749	0.994
V42 (p.u.)	0.94	1.06	1.0024	1.0221	0.9852	T95 (p.u.)	0.9	1.1	1.0023	0.9331	0.9302
V46 (p.u.)	0.94	1.06	1.0052	1.0405	1.0592	T102 (p.u.)	0.9	1.1	0.9472	0.9077	0.9474
V49 (p.u.)	0.94	1.06	1.0183	1.0007	1.0598	T107 (p.u.)	0.9	1.1	0.9005	1.0011	1.0326
V54 (p.u.)	0.94	1.06	0.9659	1.0514	0.9951	T127 (p.u.)	0.9	1.1	0.9612	0.9715	0.9519
V55 (p.u.)	0.94	1.06	0.9631	0.9669	1.013	QC5 (MVAr)	−40	0	−30.85	−7.94	−14.55
V56 (p.u.)	0.94	1.06	0.9696	1.0194	0.9435	QC34 (MVAr)	0	14	9.75	3.98	10.81
V59 (p.u.)	0.94	1.06	0.9987	1.0321	0.9602	QC37 (MVAr)	−15	0	−7.37	−0.0036	−8.14
V61 (p.u.)	0.94	1.06	1.0134	1.0171	0.9865	QC44 (MVAr)	0	10	7.3	8.29	5.83
V62 (p.u.)	0.94	1.06	1.0154	0.9607	1.0434	QC45 (MVAr)	0	10	2.9	9.01	8.96
V65 (p.u.)	0.94	1.06	1.0416	1.0426	1.0097	QC46 (MVAr)	0	10	0.84	5.12	4.92
V66 (p.u.)	0.94	1.06	1.0369	1.0503	1.0047	QC48 (MVAr)	0	10	6.46	0.23	3
V69 (p.u.)	0.94	1.06	1.0457	0.956	0.9812	QC74 (MVAr)	0	12	2.03	2.06	4.17
V70 (p.u.)	0.94	1.06	1.0289	0.9878	0.996	QC79 (MVAr)	0	20	2.84	16.65	7.75

Table 17 continued

Control parameters	Min.	Max.	Case 17	Case 18	19	Control parameters	Min.	Max.	Case 17	Case 18	19
V72 (p.u.)	0.94	1.06	1.0197	0.9603	0.9888	QC82 (MVAr)	0	20	17.49	13.94	19.05
V73 (p.u.)	0.94	1.06	1.0355	1.034	1.0121	QC83 (MVAr)	0	10	6	7.03	8.79
V74 (p.u.)	0.94	1.06	1.0085	1.025	0.9753	QC105 (MVAr)	0	20	16.59	9.19	8.96
V76 (p.u.)	0.94	1.06	1.0131	1.034	1.0327	QC107 (MVAr)	0	6	2.39	5.94	1.24
V77 (p.u.)	0.94	1.06	1.0255	1.0071	0.9813	QC110 (MVAr)	0	6	1.24	3.29	2.01
V80 (p.u.)	0.94	1.06	1.0324	1.0111	1.0434	Optimal location of SVC1			NA	NA	NA
V85 (p.u.)	0.94	1.06	1.0355	1.0272	1.0564	Optimal location of SVC2			NA	NA	NA
V87 (p.u.)	0.94	1.06	1.0266	1.0223	0.9866	QSVC1 (MVAr)	− 10	10	NA	NA	NA
V89 (p.u.)	0.94	1.06	1.0464	1.0007	1.0077	QSVC2 (MVAr)	− 10	10	NA	NA	NA
V90 (p.u.)	0.94	1.06	0.9882	1.0399	0.9608						
Objective function						Case-17		Case-18		Case-19	
APL (MW)						**124.77**		167.876		176.867	
AVD (p.u.)						0.5643		**0.35652**		0.6607	
L-index						2.1201		1.9807		**1.2404**	

Bold values are signifying the optimal results of single and multi-objective functions for different cases of the proposed work

Table 18 Simulation results of case studies with fixed loading (100%) for the IEEE 118-bus system (with SVC)

Control parameters	Min.	Max.	Case 20	Case 21	22	Control parameters	Min.	Max.	Case 20	Case 21	22
V1 (p.u.)	0.94	1.06	1.0082	1.0093	1.0251	V91 (p.u.)	0.94	1.06	1.0243	0.9863	1.0551
V4 (p.u.)	0.94	1.06	1.0367	1.0096	0.9685	V92 (p.u.)	0.94	1.06	1.0336	1.008	0.9677
V6 (p.u.)	0.94	1.06	1.0311	0.9986	0.9573	V99 (p.u.)	0.94	1.06	0.9892	0.996	1.0376
V8 (p.u.)	0.94	1.06	1.0538	1.019	0.9733	V100 (p.u.)	0.94	1.06	1.0175	1.0327	1.0363
V10 (p.u.)	0.94	1.06	1.0514	0.9638	1.0393	V103 (p.u.)	0.94	1.06	1.015	1.0286	0.9759
V12 (p.u.)	0.94	1.06	1.0207	1.0012	0.9498	V104 (p.u.)	0.94	1.06	1.0057	1.0583	0.9548
V15 (p.u.)	0.94	1.06	1.0071	1.0258	1.0514	V105 (p.u.)	0.94	1.06	1.0047	0.9908	1.0467
V18 (p.u.)	0.94	1.06	1.0206	0.957	1.0422	V107 (p.u.)	0.94	1.06	0.9989	1.0565	1.0518
V19 (p.u.)	0.94	1.06	1.0088	1.0244	0.9719	V110 (p.u.)	0.94	1.06	1.0069	1.0172	0.9871
V24 (p.u.)	0.94	1.06	1.0212	1.0202	0.9889	V111 (p.u.)	0.94	1.06	1.023	1.0558	1.011
V25 (p.u.)	0.94	1.06	1.0549	1.0014	1.0264	V112 (p.u.)	0.94	1.06	0.9987	1.0437	1.0341
V26 (p.u.)	0.94	1.06	1.0523	0.9604	0.9509	V113 (p.u.)	0.94	1.06	1.0271	0.9589	1.0441
V27 (p.u.)	0.94	1.06	1.0106	0.9905	0.969	V116 (p.u.)	0.94	1.06	1.0108	0.9767	1.0401
V31 (p.u.)	0.94	1.06	0.9935	1.0098	1.019	T8 (p.u.)	0.9	1.1	0.9779	1.0845	0.964
V32 (p.u.)	0.94	1.06	1.0043	1.0114	1.0084	T32 (p.u.)	0.9	1.1	1.0458	1.0285	1.0576
V34 (p.u.)	0.94	1.06	1.0201	1.0047	1.0554	T36 (p.u.)	0.9	1.1	0.9949	0.9756	1.0043
V36 (p.u.)	0.94	1.06	1.0256	0.9974	1.0354	T51 (p.u.)	0.9	1.1	0.9606	1.0021	1.0956
V40 (p.u.)	0.94	1.06	1.0028	1.0127	0.9889	T93 (p.u.)	0.9	1.1	0.9398	1.017	1.0602
V42 (p.u.)	0.94	1.06	1.0075	0.9671	0.9497	T95 (p.u.)	0.9	1.1	1.0001	0.9996	0.9643
V46 (p.u.)	0.94	1.06	0.9977	1.0348	1.0552	T102 (p.u.)	0.9	1.1	0.9207	0.9971	1.0621

Table 18 continued

Control parameters	Min.	Max.	Case 20	Case 21	22	Control parameters	Min.	Max.	Case 20	Case 21	22
V49 (p.u.)	0.94	1.06	1.0293	1.0204	1.0596	T107 (p.u.)	0.9	1.1	0.9674	1.0761	0.9875
V54 (p.u.)	0.94	1.06	0.9955	1.0323	1.0047	T127 (p.u.)	0.9	1.1	1.0398	0.9895	0.9717
V55 (p.u.)	0.94	1.06	0.9946	0.9914	1.0475	QC5 (MVAr)	−40	0	−37.01	−3.93	−10.19
V56 (p.u.)	0.94	1.06	0.9941	1.0083	1.0063	QC34 (MVAr)	0	14	2.24	13.28	5.48
V59 (p.u.)	0.94	1.06	1.0201	0.9546	0.9666	QC37 (MVAr)	−15	0	−1.68	−11.65	−15
V61 (p.u.)	0.94	1.06	1.0179	1.0028	1.0352	QC44 (MVAr)	0	10	5.84	5.46	9.38
V62 (p.u.)	0.94	1.06	1.0078	1.0295	0.9803	QC45 (MVAr)	0	10	5.18	9.95	4.06
V65 (p.u.)	0.94	1.06	1.0082	1.0377	0.9649	QC46 (MVAr)	0	10	8.79	0.87	3.36
V66 (p.u.)	0.94	1.06	1.0513	1.0003	1.0313	QC48 (MVAr)	0	10	2.89	4.26	4.87
V69 (p.u.)	0.94	1.06	1.0401	0.9504	1.0544	QC74 (MVAr)	0	12	2.65	0.29	0.14
V70 (p.u.)	0.94	1.06	0.9948	0.9962	1.0319	QC79 (MVAr)	0	20	19.52	11.17	13.55
V72 (p.u.)	0.94	1.06	0.9898	0.9725	1.019	QC82 (MVAr)	0	20	17.23	15.65	1.95
V73 (p.u.)	0.94	1.06	1.0029	1.0147	0.9832	QC83 (MVAr)	0	10	8.29	9.42	6.23
V74 (p.u.)	0.94	1.06	0.9728	1.028	0.9411	QC105 (MVAr)	0	20	0.4	13.39	14.59
V76 (p.u.)	0.94	1.06	1.001	1.0167	0.9752	QC107 (MVAr)	0	6	5.94	4.61	3.97
V77 (p.u.)	0.94	1.06	1.0075	1.0026	0.9467	QC110 (MVAr)	0	6	2.75	2.77	4.89
V80 (p.u.)	0.94	1.06	1.0114	1.0157	1.0033	Optimal location of SVC1			57	57	41
V85 (p.u.)	0.94	1.06	1.0334	1.0203	0.945	Optimal location of SVC2			101	95	79
V87 (p.u.)	0.94	1.06	1.0433	0.991	0.9478	QSVC1 (MVAr)	−10	10	9.8097	8.9867	9.1107
V89 (p.u.)	0.94	1.06	1.0556	0.9983	0.973	QSVC2 (MVAr)	−10	10	9.7863	7.4429	8.0098
V90 (p.u.)	0.94	1.06	1.0366	0.9854	1.0144						
Objective function						Case-20		Case-21		Case-22	
APL(MW)						**122.56**		161.4508		172.0927	
AVD (p.u.)						0.5278		**0.32437**		0.6498	
L-index						2.0401		1.7893		**1.1103**	

Bold values are signifying the optimal results of single and multi-objective functions for different cases of the proposed work

- The convergence characteristics in Fig. 10 depicts that MMKE approach converge in 30 iterations which is 27% faster than CODTBO, 33% than DTBO and 67% faster than MFO. It justifies the exploration capability of the proposed technique to reach to the global optimal solution in less computational time with overcoming the local optimal problem.
- The Friedman test rank or proposed MMKE is more than critical value which signifies more rejection of null hypothetical and closed to actual value for MMKE.
- It has also been observed from the simulation study that after incorporating FACTs devices, the voltage profile of the transmission line has been improved.
- The proposed MMKE approach tested on IEEE 118 bus system for ORPD and ORPD with FACTS devices provides optimal solution on APL, AVD and L-index. Hence, it exhibits that the suggested approach effectively copes with the large complicated power system.

In future higher ordered IEEE standard networks can be examined rigorously.

Appendix

See Table 19.

Table 19 Appendix: generator data for IEEE 30 bus system

Bus no	Pg min	max	Qg min	max	Setting of thermal unit Case 1–8	Case 9–16
1	50	200	− 20	150	Swing	Swing
2	20	80	− 20	60	75	75
5 (thermal)	15	50	− 15	62.5	40	–
5 (wind I)	0	75	− 30	35		Variable
8	10	35	− 15	48.7	30	30
11 (thermal)	10	30	− 10	40	25	–
11 (PV)	0	50	− 20	25		Variable
13 (thermal)	12	40	− 15	44.7	30	–
13 (wind II)	0	45	− 20	35		Variable
13 (Tidal)	0	5	− 10	20		Variable

Author Contributions Manuscript is written by: Mr Sabyasachi Gupta Table and Figures is done by: Dr Tushnik sarkar and Dr Chandan Paul Programming part is done by: Dr Susanta Dutta and Dr Provas kumar Roy. Final check and correction is made by: Dr Provas kumar Roy.

Data availability No datasets were generated or analysed during the current study.

Declarations

Conflict of interest The authors declare that they have no Conflict of interest.

References

1. Enes Yalcin M, Taplamacioglu Cengiz, Ertuğrul ÇAM (2019) The adaptive chaotic symbiotic organisms search algorithm proposal for optimal reactive power dispatch problem in power systems. Electrica 19(1):37–47
2. Yasir M, Rahimdad K, Farman U, Rehman AU, Aslam MS, Raja MAZ (2020) Design of fractional swarming strategy for solution of optimal reactive power dispatch. Neural Comput Appl 32:10501–10518
3. Ali MH, Soliman AMA, Abdeen M, Kandil T, Abdelaziz AY, El-Shahat A (2023) A novel stochastic optimizer solving optimal reactive power dispatch problem considering renewable energy resources. Energies 16(4):1562
4. Gafar MG, El-Sehiemy RA, Hasanien HM (2019) A novel hybrid fuzzy-JAYA optimization algorithm for efficient ORPD solution. IEEE Access 7:182078–182088
5. Salimin RH, Ismail Musirin Z, Hamid A, Harun AF, Suliman SI, Suyono H, Hasanah RN (2020) Multi cases optimal reactive power dispatch using evolutionary programming. Indones J Electr Eng Comput Sci 17:662–670
6. Jamal R, Zhang J, Men B, Khan NH, Ebeed M, Kamel S (2023) Solution to the deterministic and stochastic optimal reactive power dispatch by integration of solar, wind-hydro powers using modified artificial hummingbird algorithm. Energy Rep 9:4157–4173
7. Muhammad Y, Khan R, Raja MAZ, Ullah F, Chaudhary NI, He Y (2020) Solution of optimal reactive power dispatch with facts devices: a survey. Energy Rep 6:2211–2229
8. Li J, Tianguang L, Yi X, An M, Hao R (2024) Energy systems capacity planning under high renewable penetration considering concentrating solar power. Sustain Energy Technol Assess 64:103671
9. Li J, Tianguang L, Yi X, Hao R, Qian Ai Yu, Guo MA, Wang S, He X, Li Y (2024) Concentrated solar power for a reliable expansion of energy systems with high renewable penetration considering seasonal balance. Renew Energy 226:120089

10. ElSayed SK, Elattar EE (2021) Slime mold algorithm for optimal reactive power dispatch combining with renewable energy sources. Sustainability 13(11):5831
11. Mugemanyi S, Zhaoyang Q, Rugema FX, Dong Y, Bananeza C, Wang L (2020) Optimal reactive power dispatch using chaotic bat algorithm. IEEE Access 8:65830–65867
12. Jamal R, Men B, Khan NH (2020) A novel nature inspired meta-heuristic optimization approach of GWO optimizer for optimal reactive power dispatch problems. IEEE Access 8:202596–202610
13. Abdel-Fatah S, Ebeed M, Kamel S (2019) Optimal reactive power dispatch using modified sine cosine algorithm. In: *2019 International conference on innovative trends in computer engineering (ITCE)*, p 510–514. IEEE
14. Biswas PP, Suganthan PN, Mallipeddi R, Amaratunga GAJ (2019) Optimal reactive power dispatch with uncertainties in load demand and renewable energy sources adopting scenario-based approach. Appl Soft Comput 75:616–632
15. Aljohani TM, Ebrahim AF, Mohammed O (2019) Single and multi-objective optimal reactive power dispatch based on hybrid artificial physics-particle swarm optimization. Energies 12(12):2333
16. Li Z, Cao Y, Van Dai L, Yang X, Nguyen TT (2019) Finding solutions for optimal reactive power dispatch problem by a novel improved antlion optimization algorithm. Energies 12(15):2968
17. Mahdad B, Kamel S (2019) New strategy based modified SALP swarm algorithm for optimal reactive power planning: a case study of the Algerian electrical system (114 bus). IET Gener Transm Distrib 13(20):4523–4540
18. Salah Kamel, Said Abdel-Fatah, Mohamed Ebeed, Juan Yu, Kaigui Xie, and Chenyu Zhao (2019) Solving optimal reactive power dispatch problem considering load uncertainty. In *2019 IEEE innovative smart grid technologies-Asia (ISGT Asia)*, p 1335–1340. IEEE
19. Ebeed M, Alhejji A, Kamel S, Jurado F (2020) Solving the optimal reactive power dispatch using marine predators algorithm considering the uncertainties in load and wind-solar generation systems. Energies 13(17):4316
20. Thang Trung Nguyen and Dieu Ngoc Vo (2020) Improved social spider optimization algorithm for optimal reactive power dispatch problem with different objectives. Neural Comput Appl 32(10):5919–5950
21. Ettappan M, Vimala V, Ramesh Subramanian, Thiruppathy VK (2020) Optimal reactive power dispatch for real power loss minimization and voltage stability enhancement using artificial bee colony algorithm. Microprocess Microsyst 76:103085
22. Zhou Y, Zhang J, Yang X, Ling Y (2020) Optimal reactive power dispatch using water wave optimization algorithm. Op Res 20:2537–2553
23. Das T, Roy R, Mandal KK, Mondal S, Mondal S, Hait P, Das MK (2020) Optimal reactive power dispatch incorporating solar power using jaya algorithm. In: *Computational advancement in communication circuits and systems: proceedings of ICCACCS 2018*, p 37–48. Springer
24. Shaheen MAM, Hasanien HM, Alkuhayli A (2021) A novel hybrid GWO-PSO optimization technique for optimal reactive power dispatch problem solution. Ain Shams Eng J 12(1):621–630
25. Wei Y, Zhou Y, Luo Q, Deng W (2021) Optimal reactive power dispatch using an improved slime mould algorithm. Energy Rep 7:8742–8759
26. Yapici H (2021) Solution of optimal reactive power dispatch problem using pathfinder algorithm. Eng Optim 53(11):1946–1963
27. Elsayed SK, Kamel S, Selim A, Ahmed M (2021) An improved heap-based optimizer for optimal reactive power dispatch. IEEE Access 9:58319–58336
28. Mouassa S, Jurado F, Bouktir T, Raja MAZ (2021) Novel design of artificial ecosystem optimizer for large-scale optimal reactive power dispatch problem with application to Algerian electricity grid. Neural Comput Appl 33:7467–7490
29. Duong V-T, Nguyen T-T, Duong T-L, Truong A-V (2021) Optimal reactive power dispatch using sunflower algorithm. In: *2021 International conference on system science and engineering (ICSSE)*, p 422–426. IEEE
30. Lenin K (2021) Hybridization of genetic particle swarm optimization algorithm with symbiotic organisms search algorithm for solving optimal reactive power dispatch problem. J Appl Sci Eng Technol Edu 3(1):12–21
31. Shanono IH, Mahmud MA, Abdullah NRH, Mustafa M, Samad R, Pebrianti D, Muhammad A (2021) Optimal reactive power dispatch solution by loss minimisation using dragonfly optimization algorithm. In: *Proceedings of the 11th National Technical Seminar on Unmanned System Technology 2019: NUSYS'19*, p 1083–1103. Springer
32. Abd-El AM, Wahab SK, Hassan MH, Mosaad MI, AbdulFattah TA (2022) Optimal reactive power dispatch using a chaotic turbulent flow of water-based optimization algorithm. Mathematics 10(3):346
33. Anil Kumar PG, Devaraj D et al (2022) Hybrid CAC-DE in optimal reactive power dispatch (ORPD) for renewable energy cost reduction. Sustain Comput Inform Syst 35:100688
34. Gupta SK, Kumar L, Kar MK, Kumar S (2022) Optimal reactive power dispatch under coordinated active and reactive load variations using facts devices. Int J Syst Assur Eng Manag 13(5):2672–2682
35. Waleed U, Haseeb A, Ashraf MM, Siddiq F, Rafiq M, Shafique M (2022) A multiobjective artificial-hummingbird-algorithm-based framework for optimal reactive power dispatch considering renewable energy sources. Energies 15(23):9250
36. Rani N, Malakar T (2022) A reactive power reserve constrained optimum reactive power dispatch using coronavirus herd immunity optimizer. Electric Power Compon Syst 50(4–5):223–244
37. Zhaoyang Q, Dong Y, Mugemanyi S, Tong Yu, Bo X, Li H, Li Y, Rugema FX, Bananeza C (2022) Dynamic exploitation gaussian bare-bones bat algorithm for optimal reactive power dispatch to improve the safety and stability of power system. IET Renew Power Gener 16(7):1401–1424
38. Gami F, Alrowaili ZA, Ezzeldien M, Ebeed M, Kamel S, Oda ES, Mohamed SA (2022) Stochastic optimal reactive power dispatch at varying time of load demand and renewable energy resources using an efficient modified jellyfish optimizer. Neural Comput Appl 34(22):20395–20410
39. Long H, Liu S, Chen T, Tan H, Wei J, Zhang C, Chen W (2022) Optimal reactive power dispatch based on multi-strategy improved aquila optimization algorithm. *IAENG Int J Comput Sci*, 49(4)
40. Ucheniya R, Saraswat A, Siddiqui SA (2022) Decision making under wind power generation and load demand uncertainties: a two-stage stochastic optimal reactive power dispatch problem. Int J Modell Simul 42(1):47–62
41. Sarhan S, Shaheen A, El-Sehiemy R, Gafar M (2023) An augmented social network search algorithm for optimal reactive power dispatch problem. Mathematics 11(5):1236
42. Abd-El Wahab AM, Kamel S, Hassan MH, Domínguez-García JL, Nasrat L (2023) Jaya-aeo: an innovative hybrid optimizer for reactive power dispatch optimization in power systems. *Electric Power Compon Syst*, 1–23
43. Sulaiman MH, Mustaffa Z, Aliman O, Saari MM (2023) Improved barnacles mating optimizer for loss minimization problem in optimal reactive power dispatch. In: *2023 IEEE 13th Symposium on computer applications and industrial electronics (ISCAIE)*, p 51–55. IEEE
44. Nadimi-Shahraki MH, Taghian S, Zamani H, Mirjalili S, Elaziz MA (2023) MMKE: multi-trial vector-based monkey king evolu-

tion algorithm and its applications for engineering optimization problems. Plos ONE 18(1):e0280006
45. Meng Z, Pan J-S (2016) Monkey king evolution: a new memetic evolutionary algorithm and its application in vehicle fuel consumption optimization. Knowl Based Syst 97:144–157
46. Rambabu M, Nagesh Kumar GV, Sivanagaraju S (2019) Optimal power flow of integrated renewable energy system using a thyristor controlled seriescompensator and a grey-wolf algorithm. Energies 12(11):2215
47. Duman S, Li J, Lei W, Guvenc U (2020) Optimal power flow with stochastic wind power and facts devices: a modified hybrid PSOGSA with chaotic maps approach. Neural Comput Appl 32:8463–8492
48. Abdullah M, Javaid N, Khan IU, Khan ZA, Chand A, Ahmad N (2020) Optimal power flow with uncertain renewable energy sources using flower pollination algorithm. In: *Advanced information networking and applications: proceedings of the 33rd international conference on advanced information networking and applications (AINA-2019)* 33, p 95–107. Springer
49. Duman S, Akbel M, Kahraman HT (2021) Development of the multi-objective adaptive guided differential evolution and optimization of the MO-ACOPF for wind/PV/tidal energy sources. Appl Soft Comput 112:107814
50. Khan NH, Jamal R, Ebeed M, Kamel S, Zeinoddini-Meymand H, Zawbaa HM (2022) Adopting scenario-based approach to solve optimal reactive power dispatch problem with integration of wind and solar energy using improved marine predator algorithm. Ain Shams Eng J 13(5):101726
51. Tanabe R, Fukunaga A (2013) Success-history based parameter adaptation for differential evolution. In: *2013 IEEE congress on evolutionary computation*, p 71–78. IEEE
52. Growe-Kuska N, Heitsch H, Romisch W (2003) Scenario reduction and scenario tree construction for power management problems. In: *2003 IEEE Bologna power tech conference proceedings*, 3: 7. IEEE
53. Paul C, Sarkar T, Dutta S, Roy PK (2024) Multi-objective combined heat and power with wind-solar-EV of optimal power flow using hybrid evolutionary approach. Electr Eng 106(2):1619–1653
54. Hazra S, Roy PK, Paul C (2024) State of the art for moth-flame optimization applied electric vehicles–solar–wind–hydro–thermal power system. *Electr Eng*, p 1–27
55. Roy R, Das T, Mandal KK (2021) Optimal reactive power dispatch using a novel optimization algorithm. J Electr Syst Inf Technol 8:1–24